© 2020. Published by The Company of Biologists Ltd | Journal of Cell Science (2020) 133, jcs236265. doi:10.1242/jcs.236265

RESEARCH ARTICLE

Lamin A/C modulates spatial organization and function of the Hsp70 gene locus via nuclear myosin I

Roopali Pradhan, Muhunden Jayakrishnan Nallappa and Kundan Sengupta*

ABSTRACT

The structure–function relationship of the nucleus is tightly regulated, especially during heat shock. Typically, heat shock activates molecular chaperones that prevent protein misfolding and preserve genome integrity. However, the molecular mechanisms that regulate nuclear structure–function relationships during heat shock remain unclear. Here, we show that lamin A and C (hereafter lamin A/C; both lamin A and C are encoded by *LMNA*) are required for heat-shock-mediated transcriptional induction of the Hsp70 gene locus (HSPA genes). Interestingly, lamin A/C regulates redistribution of nuclear myosin I (NM1) into the nucleus upon heat shock, and depletion of either lamin A/C or NM1 abrogates heat-shock-induced repositioning of Hsp70 gene locus away from the nuclear envelope. Lamins and NM1 also regulate spatial positioning of the SC35 (also known as SRSF2) speckles – important nuclear landmarks that modulates Hsp70 gene locus expression upon heat shock. This suggests an intricate crosstalk between nuclear lamins, NM1 and SC35 organization in modulating transcriptional responses of the Hsp70 gene locus during heat shock. Taken together, this study unravels a novel role for lamin A/C in the regulation of the spatial dynamics and function of the Hsp70 gene locus upon heat shock, via the nuclear motor protein NM1.

This article has an associated First Person interview with the first author of the paper.

KEY WORDS: Heat shock, Hsp70, Lamin, Nuclear Myosin I, SC35, Transcription

INTRODUCTION

It is of paramount importance to maintain the integrity of the nucleus and the genome, especially when cells encounter external stress. Cells have diverse mechanisms for their survival even when subject to wide variations in temperature (Pauli et al., 1992; Tanguay, 1983). Heat-shock proteins such as members of the Hsp70 and Hsp90 families are synthesized in response to elevated temperatures (Richter et al., 2010; Velichko et al., 2013). These molecular chaperones bind to DNA to protect it from single stranded breaks and proteins to prevent them from misfolding (Morimoto, 1998; Richter et al., 2010). Upon heat shock, the transcription factor heat-shock factor 1 (HSF1) is unbound from its interactors, such as Hsp90 and Hsp70 (otherwise expressed at low basal levels), undergoes autophosphorylation, translocates into the nucleus and binds to the promoters of heat-shock genes, facilitating their expression (Baler et al., 1993; Demirovic et al., 2014; Jolly et al., 1997; Sarge et al., 1993).

Upon heat-shock, five major families of heat-shock proteins are induced namely – HSPA (Hsp70 family; note herein Hsp70 refers to the products of the three closely related genes *HSPA1A*, *HSPA1B* and *HSPA1L*), HSPB (small HSP family), HSPC (Hsp90 family), HSPD (Hsp60 family) and HSPH (large HSP family) (Daugaard et al., 2007; Stetler et al., 2010). HSF1 binds to the promoters of Hsp70 gene locus and induces its actin-mediated directional movement toward nuclear speckles, which are enriched in transcription factors and in close proximity to the locus; contact with speckles induces transcriptional upregulation of Hsp70 gene locus (Daugaard et al., 2007; Hu et al., 2010; Jolly et al., 1999; Khanna et al., 2014; Kim et al., 2020). After attenuation of heat shock, HSF1–Hsp70 dimers are reformed, inactivating HSF1, completing the negative feedback loop (Demirovic et al., 2014; Morimoto, 1998; Sarge et al., 1993). During the heat-shock response, active translocation of Hsp70 into the nucleus is mediated by Hikeshi, a nuclear import carrier (Imamoto and Kose, 2012). Hsp70 is implicated in regulating rDNA transcription during heat shock and in maintaining cell viability during recovery post heat shock (Kose and Imamoto, 2014; Kose et al., 2012; Yanoma et al., 2017).

How factors that maintain nuclear architecture and function respond to heat shock is unclear. Nuclear lamins maintain structural and functional integrity of the nucleus along with their interactors (Dechat et al., 2010; Prokocimer et al., 2009; Shimi et al., 2008; Wilson and Foisner, 2010; Zastrow et al., 2004). In *Drosophila* Schneider 2 cells, heat shock converts lamin Dm2 into lamin Dm1 by dephosphorylation (Smith and Fisher, 1984; Smith et al., 1987). Exposure of Ehrlich Ascites tumor cells to heat shock, leads to the dephosphorylation of lamin A and C (hereafter lamin A/C; both lamin A and C are encoded by *LMNA*), further affecting the structural stability of the nucleoskeletal meshwork (Krachmarov and Traub, 1993). Lamin B is a heat-shock-responsive protein and its expression is upregulated at 45.5°C in U-1 melanoma and HeLa cells (Dynlacht et al., 1999; Falloon and Dynlacht, 2002; Zhu et al., 1999). Interestingly, small heat-shock proteins (sHsps) like αB-crystallin and Hsp25 (also known as HSPB1) colocalize with lamin A/C in the nucleoplasm upon heat shock in C2C12 myoblast cells (Willsie and Clegg, 2002). Analyses of mouse pituitary gland tissue using mass spectrometry coupled with isobaric tags for relative and absolute quantitation (iTRAQ) shows that heat stress enhances expression of pre-lamin A/C, lamin B1, vimentin and keratin (Memon et al., 2016). Taken together, these results suggest a regulatory crosstalk between the heat-shock response and nuclear lamins.

Nuclear proteins such as BAF, LAP2α (lamin-interacting proteins) and the nucleolar protein NPM1 are altered in their localization and dynamics during heat stress across cell types (Bar et al., 2014; Snyers and Schöfer, 2008; Vanderwaal et al., 2009; Willsie and Clegg, 2002). The mechanisms by which the heat-shock response is transduced and regulated by nuclear lamins are unclear.

Biology, Main Building, First Floor, Room B-216, Indian Institute of Science Education and Research (IISER), Pune 411008, India.

*Author for correspondence (kunsen@iiserpune.ac.in)

K.S., 0000-0002-9936-2284

Received 11 July 2019; Accepted 13 January 2020

Journal of Cell Science (2020) 133, jcs236265. doi:10.1242/jcs.236265

Altered localization of proteins that maintain nuclear architecture can potentially modulate perception of heat shock by the nucleus depending on the duration and temperature of the treatment. For instance, fibroblasts derived from Hutchinson–Gilford progeria syndrome (HGPS) patients with the lamin A/C mutation (G608G) are hypersensitive to heat stress (Paradisi et al., 2005). It is well established that global transcriptional changes are elicited during heat stress (Kantidze et al., 2015; Mahat et al., 2016). Lamins can modulate the Polycomb repressive complex and further fine-tune the transcriptome during heat shock (Cesarini et al., 2015; Marullo et al., 2016).

Here, we examined the role of nuclear lamins in regulating the heat-shock response. We show that subjecting cells to heat shock significantly upregulates lamin B1 and lamin A levels. Lamins are required for heat-shock-induced upregulation of the heat-shock gene *HSPA1A*, which is a part of the Hsp70 gene locus. Remarkably, depletion of lamin A/C, but not the B-type lamins, inhibits movement of the Hsp70 gene locus toward the nuclear interior and nuclear translocation of Hsp70 protein from the cytoplasm upon thermal stress. Lamin A/C also regulates the localization of the nuclear motor protein nuclear myosin I (NM1, myosin 1c isoform B), into the nucleus. NM1 repositions the Hsp70 gene locus upon heat shock, as NM1 knockdown or inhibition of NM1 activity attenuates *HSPA1A* gene expression and impairs movement of the Hsp70 gene locus toward the nuclear interior. Furthermore, lamins and NM1 modulate the spatial organization of the SC35 nuclear speckles that induce Hsp70 gene locus expression upon heat shock. This suggests an intricate crosstalk between nuclear lamins, NM1 and SC35 organization in modulating transcriptional responses of the Hsp70 gene locus during heat shock. Taken together, this study unravels a novel role for lamin A/C in the regulation of the spatial dynamics and expression of the Hsp70 gene locus upon heat shock.

RESULTS

Induction and monitoring the heat-shock response in single cells

Cells have evolved ingenious mechanisms to counter extraneous stressors such as heat shock. Typically, cells maintain biochemical and cellular homeostasis at an optimal temperature of 37°C. Transferring cells to restrictive temperatures of 42°C, triggers the heat-shock response, wherein heat-shock proteins are expressed that counter the detrimental effects of elevated temperature on cells (Morimoto, 1998; Richter et al., 2010; Yanoma et al., 2017).

We examined induction of the heat-shock response in diploid colorectal cancer cells (DLD-1) by monitoring expression levels of the heat-shock gene *HSPA1A* and the subcellular localization of the heat-shock protein Hsp70, respectively. We subjected cells to increasing durations of heat shock at 42°C (identical time-points at 37°C served as control), followed by quantitative real-time RT-PCR (qRT-PCR) to quantify transcript levels of the *HSPA1A* gene (Fig. S1A). *HSPA1A* expression was significantly upregulated within ∼5–10 min of heat shock at 42°C, and the transcript levels peaked within ∼60 min (Fig. S1A). We next performed immunostaining of Hsp70 in cells subjected to heat shock for increasing durations, followed by recovery at 37°C (Fig. S1B,C). Hsp70 translocated into the nucleus in the majority of cells (∼80%) within ∼15 min of heat shock (Fig. S1D). Hsp70 showed increased expression during recovery and ∼35–40% nuclei continued to retain Hsp70 even after ∼2 h of recovery at 37°C (Fig. S1D). In contrast, hardly any cells showed Hsp70 in the nucleus at 37°C (Fig. S1C). Taken together, enhanced expression of *HSPA1A* gene and translocation of the Hsp70 protein into the nucleus underscores the induction of the heat-shock response.

Lamin A and B1 expression is upregulated during heat shock

A and B-type lamins regulate nuclear structure, function and plasticity in cells (Dechat et al., 2010; Prokocimer et al., 2009; Shimi et al., 2008; Wilson and Foisner, 2010; Zastrow et al., 2004). Notwithstanding the role of lamin B as a heat-shock-responsive protein (Dynlacht et al., 1999), the role and response of nuclear lamins upon heat shock is unclear. Small heat-shock proteins (sHsps), such as αB-crystallin and Hsp25, colocalize with lamin A/C upon heat shock in C2C12 myoblast cells (Willsie and Clegg, 2002), suggesting a potential involvement of lamins during the heat-shock response.

Here, we investigated the effect of heat shock on nuclear lamins by subjecting cells to heat shock for increasing durations, followed by recovery at 37°C in the absence of heat shock. We visualized nuclear lamins in single cells by immunofluorescence staining (Figs 1A,B and 2A,B). Lamin A levels showed a significant increase, both at the nuclear envelope and within the nucleoplasm at ∼15 min upon heat shock. This increase in lamin A levels was sustained in cells for ∼60 min of heat shock (Fig. 1C–E; Fig. S2A). Interestingly, lamin A was restored to basal levels in cells returned to 37°C for increasing durations of recovery (Fig. 1D,E). In addition, lamin B1 levels increased significantly after ∼15 min of heat shock and by ∼2-fold after 60 min at 42°C (Fig. 2C; Fig. S2A). Lamin B1 expression declined at 1 h post recovery, while the levels increased after a recovery period of 2 h, and returned to baseline levels after ∼4 h of recovery from heat shock (Fig. 2C). In contrast, lamin B2 levels showed relatively subtle changes upon heat shock, with an increase after ∼60 min at 42°C and decrease during the ∼2 h of recovery (Fig. 2D). We hardly detected lamin B1 or B2 in the nucleoplasm, consistent with a relatively enhanced nucleoplasmic localization of lamin A as compared to B-type lamins (Bridger et al., 1993; Broers et al., 1999; Fricker et al., 1997; Hozák et al., 1995; Moir et al., 2000; Pochukalina et al., 2016). In addition, the transcript levels of lamin B1 (∼2.5 fold) and lamin A (∼1.5 fold) were upregulated within ∼10 min at 42°C, while lamin B2 transcript levels were relatively unaltered until ∼60 min of heat shock (Fig. S2B). Of note, while nuclear area and circularity did not show significant changes upon heat shock, nuclear volume increased during the recovery from heat shock (Fig. S2C–E). In summary, nuclear lamin expression is altered during the activation of the heat-shock response pathway.

Lamin A/C depletion abrogates nuclear translocation of Hsp70 upon heat shock

The nuclear translocation of Hsp70 in response to heat shock prevents protein misfolding, protects cells from DNA damage and maintains cell viability during heat shock (Kose and Imamoto, 2014; Kose et al., 2012; Yanoma et al., 2017). We asked whether nuclear lamins are involved in the translocation of Hsp70 into the nucleus upon heat shock. We performed siRNA-mediated knockdowns of lamins in DLD-1 cells, followed by heat shock at 42°C for 60 min and immunostaining of the heat-shock factor Hsp70 (Fig. 3A–C; Fig. S2F). Remarkably, only a small sub-population of lamin A/C-depleted cells showed translocation of Hsp70 into the nucleus upon heat shock, while >60% of B-type lamin-depleted cells (siLaminB1, siLamin B2) showed nuclear translocation of Hsp70 upon heat shock comparable to control cells (siLacZ) (Fig. 3D). Overexpression of GFP–lamin A (siRNA resistant) rescued the nuclear translocation of Hsp70 in

Journal of Cell Science (2020) 133, jcs236265. doi:10.1242/jcs.236265

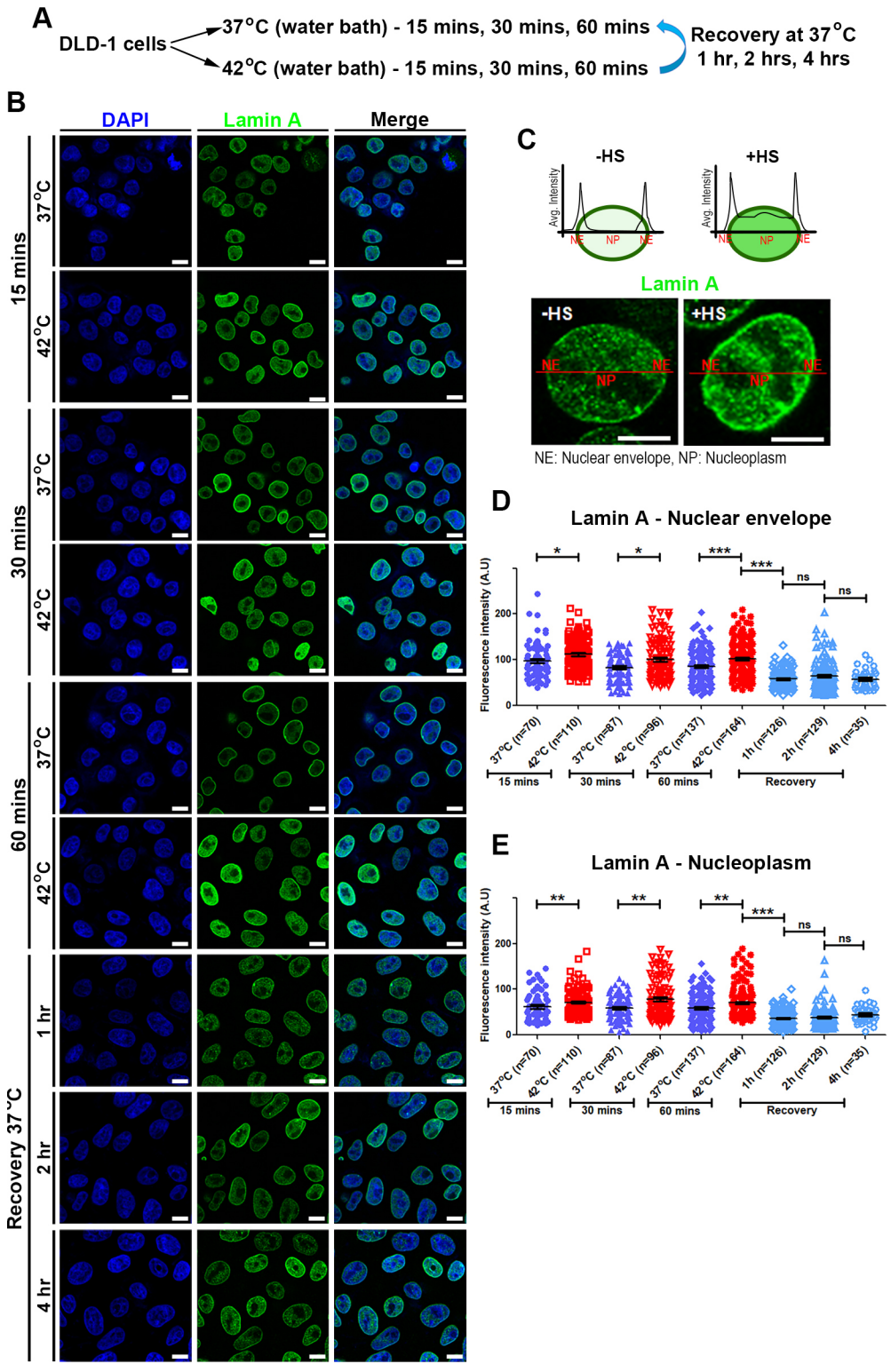

Fig. 1. Lamin A levels are upregulated upon heat shock. (A) Experimental scheme. (B) Representative mid-optical sections from confocal *z*-stacks showing lamin A immunostaining in cells exposed to heat shock at 42°C for 15, 30 and 60 min (controls at 37°C) and recovery for 1, 2 and 4 h at 37°C post 60 min heat shock. (C) Line scan analysis of a single representative nucleus with (+HS) and without (–HS) heat shock. (D,E) Dot scatter plot and mean±s.e.m. of normalized fluorescence intensities (from line scan analysis of each nucleus) for lamin A (D) nuclear envelope and (E) nucleoplasm in cells exposed to heat shock, control cells at 37°C and cells under recovery. Data are from two independent biological replicates; the number of nuclei analyzed is given on the figure (*n*). **P*<0.05; ***P*<0.001; ****P*<0.0001; ns, not significant (Mann–Whitney test). Scale bars: 10 µm.

>70% of siLamin A/C cells (depleted of endogenous lamin A/C) (Fig. 3E–G).

To address the specificity of lamin A/C in regulating nuclear import of Hsp70, and that the impaired translocation of Hsp70 upon lamin A/C depletion is not just a consequence of altered transport, we performed nuclear import assays. We employed a dexamethasone inducible reporter construct consisting of the hormone-responsive domain of glucocorticoid and GFP fused to the M9 core domain (GR2-GFP2-M9) (Hutten et al., 2009). While this construct localizes exclusively in the cytoplasm, it is imported into the nucleus following dexamethasone treatment (5 µM). Lamin A/C or lamin B2 depletion did not cause a significant difference in the nuclear import of GR2-GFP2-M9. However, lamin B1 knockdown showed a small but significant reduction in nuclear import (Fig. S3A–C). Furthermore, the depletion of nucleoporin Nup98 (an off-pore nucleoporin) showed reduced nuclear import

Journal of Cell Science (2020) 133, jcs236265. doi:10.1242/jcs.236265

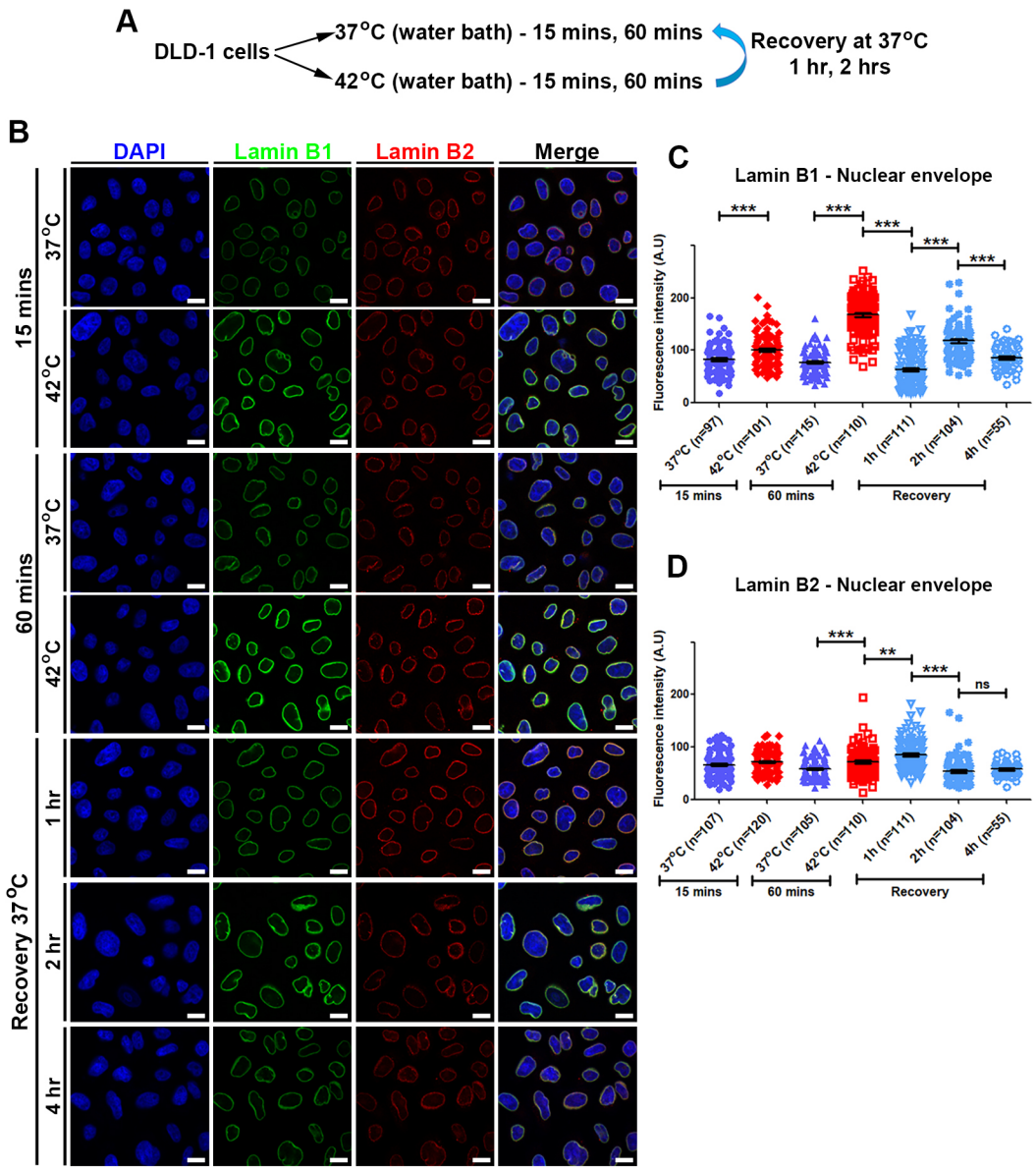

Fig. 2. Lamin B1 levels are upregulated upon heat shock. (A) Experimental scheme. (B) Representative mid-optical sections from confocal *z*-stacks showing lamin B1 and B2 immunostaining in cells exposed to heat shock at 42°C for 15 and 60 min (controls, same time points at 37°C). Recovery for 1, 2 and 4 h at 37°C post 60 min heat shock. (C,D) Dot scatter plot and mean±s.e.m. of normalized fluorescence intensities (line scan analysis of each individual nucleus) for (C) lamin B1 and (D) lamin B2, at the nuclear envelope in cells exposed to heat shock, control cells at 37°C and cells under recovery. Data are from two independent biological replicates; the number of nuclei analyzed is given on the figure (*n*). ***P*<0.01; ****P*<0.0001; ns, not significant (Mann–Whitney test). Scale bars: 10 µm.

under similar conditions, and therefore served as a positive control (Fig. S3B-C) (Labade et al., 2016). In summary, lamin A/C knockdown does not impede global nuclear import and the abrogation of the nuclear translocation of Hsp70 is a specific effect of lamin A/C depletion. Taken together, these studies show that lamin A/C modulates the import of Hsp70 into the nucleus upon heat shock.

Lamin depletion specifically attenuates the heat-shock-mediated upregulation of *HSPA1A*

We sought to examine the involvement of nuclear lamins in modulating transcriptional responses upon heat shock induction, for which we examined expression levels of *HSPA1A* (a member of the Hsp70 gene locus) upon lamin knockdown. We independently depleted lamins, followed by heat shock and performed gene expression profiling by qRT-PCR analyses of *HSPA1A* (Fig. 4A,B; Fig. S2G). Interestingly, depletion of lamins caused an ∼3-fold decrease in *HSPA1A* transcript levels at 42°C [Fig. 4B, control cells (siLacZ) showed an ∼30-fold upregulation of *HSPA1A* expression upon heat shock]. We examined the impact of lamin depletion on the expression of another member of the Hsp70 gene locus, *HSPA1L*. Lamin knockdowns showed an ∼2-fold decrease in *HSPA1L* transcript levels at 42°C [Fig. S4A,B, control cells (siLacZ) showed an ∼15-fold upregulation of *HSPA1L* expression upon heat shock]. In summary, lamins modulate *HSPA1A* and *HSPA1L* transcript levels upon heat shock.

The Hsp70 gene locus is induced in cells subjected to cadmium sulfate ($CdSO_4$)-induced metal ion stress (Polla et al., 1995). $CdSO_4$

Journal of Cell Science (2020) 133, jcs236265. doi:10.1242/jcs.236265

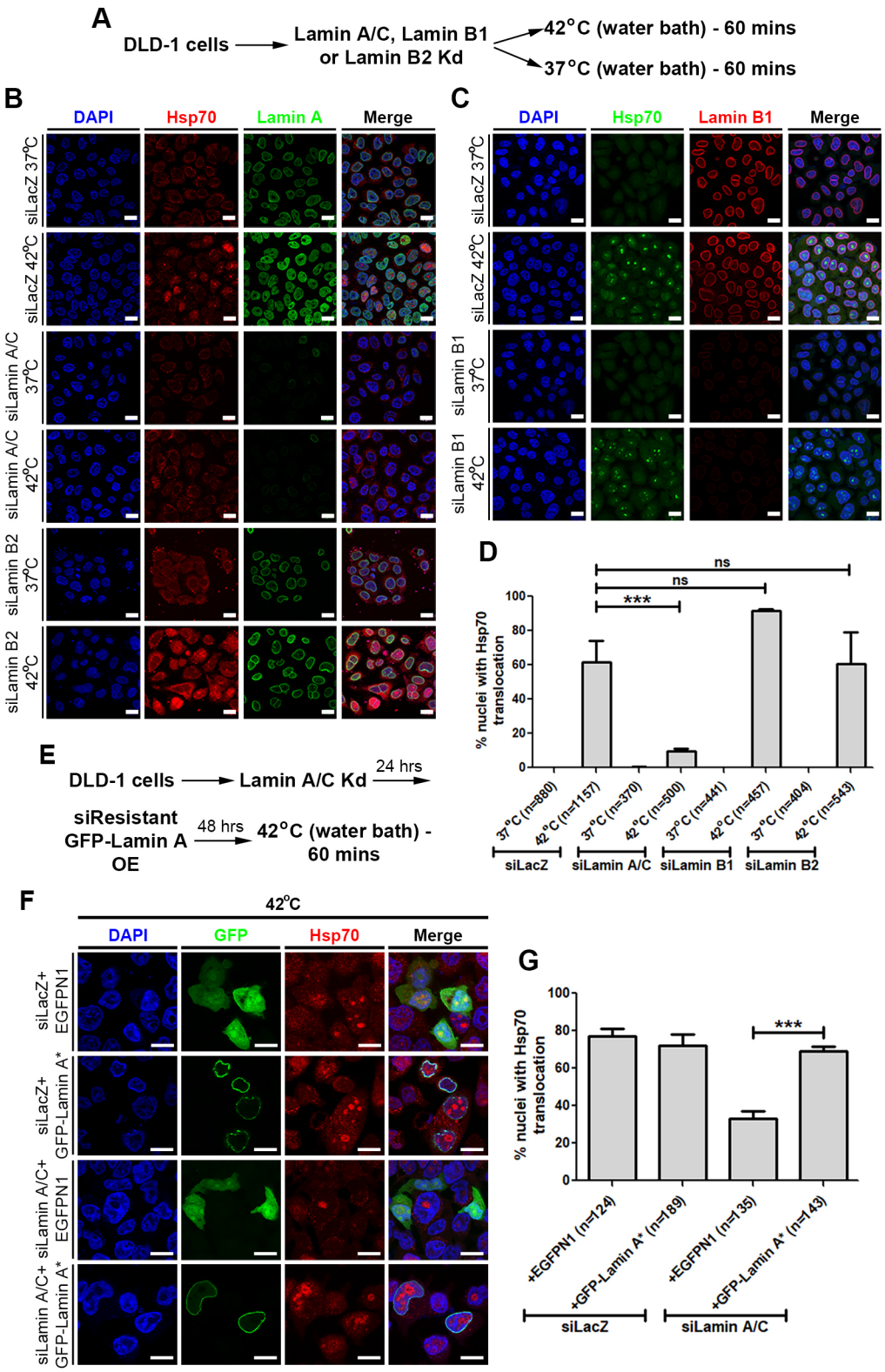

Fig. 3. Depletion of lamin A/C impairs heat-shock-induced nuclear translocation of Hsp70. (A) Experimental scheme. (B) Representative mid-optical sections from confocal *z*-stacks showing Hsp70 and lamin A immunostaining in siLacZ, siLamin A/C or siLamin B2 cells exposed to heat shock at 42°C for 60 min (controls at 37°C). (C) Representative mid-optical sections from confocal *z*-stacks showing Hsp70 and lamin B1 immunostaining in siLacZ or siLamin B1 cells exposed to heat shock at 42°C for 60 min (controls at 37°C). (D) Quantification of the mean±s.e.m. percentage of nuclei showing nuclear translocation of Hsp70 after heat shock in siLacZ, siLamin A/C, siLamin B1 and siLamin B2 cells (controls at 37°C show no nuclear translocation of Hsp70). Data from three independent biological replicates; the number of nuclei analyzed is given on the figure (*n*). ***P<0.0001; ns, not significant (Mann–Whitney test). (E) Experimental scheme. (F) Representative mid-optical sections from confocal *z*-stacks showing Hsp70 immunostaining in siLacZ or siLamin A/C cells overexpressing EGFP-N1 or siRNA-resistant (indicated by an asterisk after lamin A) GFP–lamin A and subjected to heat shock at 42°C for 60 min. (G) Quantification of the mean±s.e.m. percentage nuclei showing Hsp70 nuclear or nucleolar translocation after heat shock in siLacZ cells overexpressing EGFPN-1 or siRNA-resistant GFP-lamin A. Data are from two independent biological replicates; the number of nuclei analyzed is given on the figure (*n*). ***P<0.0001 (Mann–Whitney test). Scale bars: 10 µm.

treatment activates *HSPA1A* expression in the absence of heat shock (Hu et al., 2010). Interestingly, the same distal element near the Hsp70 gene promoter (the heat-shock element centered at −100 bp) and transcription factor (HSF1) are required for both the heat shock and metal ion stress-induced expression of the Hsp70 gene locus (Williams and Morimoto, 1990). We therefore used $CdSO_4$ treatment as an independent means to activate expression of the Hsp70 gene locus and unravel the mechanisms by which lamins exert their regulatory role in the heat-shock transcriptional response cascade. We treated cells with increasing concentrations of $CdSO_4$ for 2 h and monitored (1) *HSPA1A* and *HSPA1L* transcript levels, and (2) nuclear translocation of Hsp70 protein (Fig. S3D). Both nuclear translocation of Hsp70 and *HSPA1A* and *HSPA1L* gene expression showed a dose-dependent increase upon $CdSO_4$ treatment

Journal of Cell Science (2020) 133, jcs236265. doi:10.1242/jcs.236265

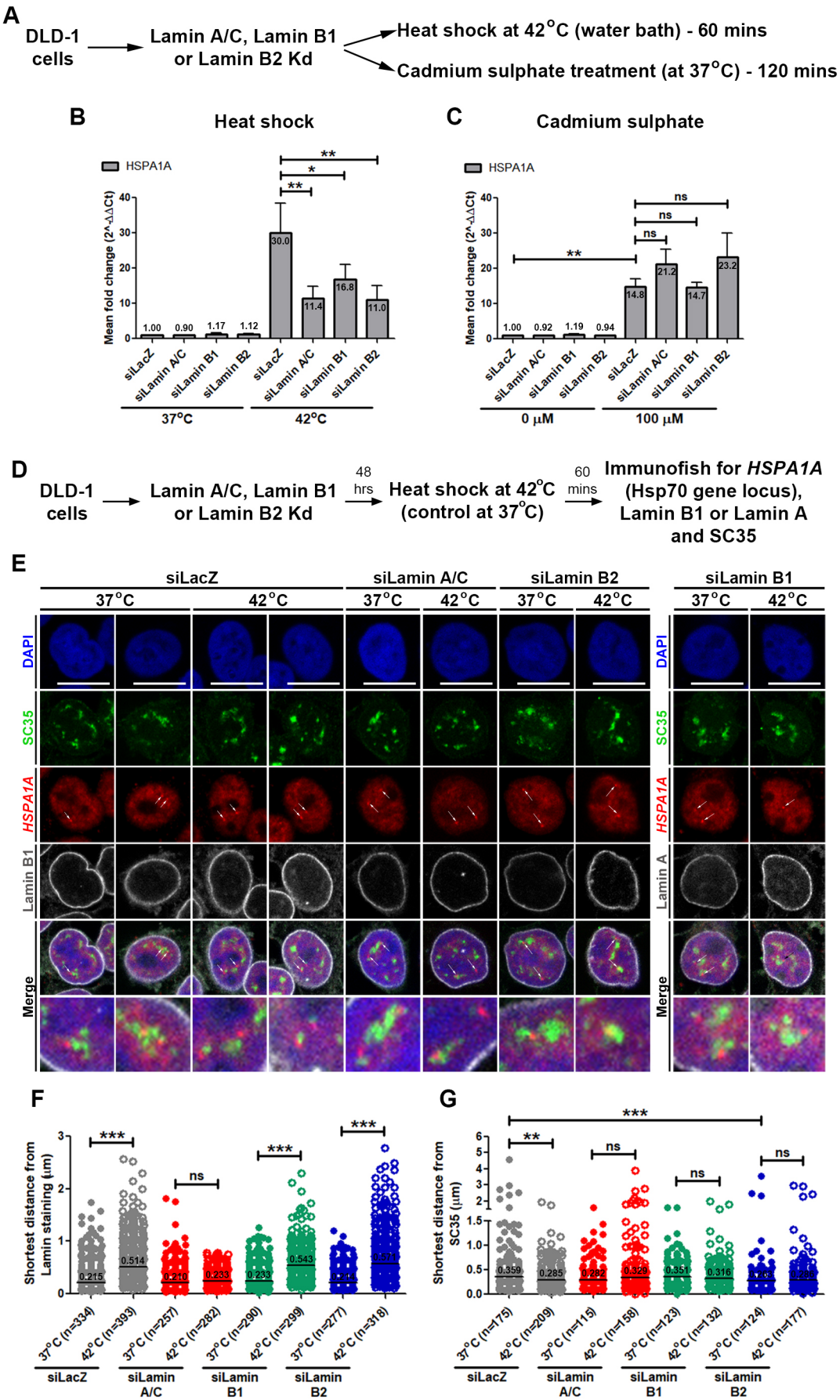

Fig. 4. See next page for legend.

Journal of Cell Science

Journal of Cell Science (2020) 133, jcs236265. doi:10.1242/jcs.236265

Fig. 4. Lamin A/C is required for heat-shock-induced expression and dynamics of the Hsp70 gene locus. (A,B) Lamin knockdown attenuates heat-shock-mediated induction of *HSPA1A*. (A) Experimental scheme. (B) Measurement of mean±s.e.m. *HSPA1A* transcript levels using qRT-PCR in siLacZ, siLamin A/C, siLamin B1 and siLamin B2 cells upon heat shock at 42°C for 60 min (controls: siRNA-treated cells at 37°C). Data from four independent biological replicates (n=12). Expression was first normalized to the internal control (GAPDH) and then to siLacZ at 37°C. *P<0.05, **P<0.001; ns, not significant (Student's t-test). (C) Measurement of mean±s.e.m. *HSPA1A* transcript levels using qRT-PCR in siLacZ, siLamin A/C, siLamin B1 and siLamin B2 cells upon 100 µM cadmium sulfate treatment at 37°C for 120 min (same volume of NFW was added in control cells). Data from three independent biological replicates (n=9). Expression was first normalized to the internal control (GAPDH) and then to siLacZ with no cadmium sulfate. **P<0.001; ns, not significant (Student's t-test). (D–G) Depletion of lamin A/C, but not B-type lamins, abrogates heat-shock-mediated movement of the Hsp70 gene locus toward the nuclear interior. (D) Experimental scheme. (E) Representative mid-optical sections from confocal z-stacks showing SC35 and lamin B1 or lamin A immunostaining, and 3D-FISH for Hsp70 gene locus (*HSPA1A*), in siLacZ, siLamin A/C, siLamin B1 and siLamin B2 cells upon heat shock at 42°C for 60 min (controls: siRNA-treated cells at 37°C). White arrows highlight specific hybridization of BAC DNA probe showing two copies of Hsp70 gene locus. (F) Dot scatter plot and median showing the shortest distance (in µm) of the Hsp70 gene loci from lamin staining in siLacZ and lamin-knockdown cells after heat shock (controls: siRNA-treated cells at 37°C). (G) Dot scatter plot and median showing the shortest distance of the Hsp70 gene loci from SC35 speckles in siLacZ, lamin knockdown cells after heat shock (controls: siRNA treated cells at 37°C). Data in F,G are from four and two independent biological replicates, respectively; the number of nuclei analyzed is given on the figure (n). **P<0.001, ***P<0.0001; ns, not significant (Mann–Whitney test). Scale bars: 10 µm.

(Fig. S3E–H). To address whether lamin depletion also affects $CdSO_4$-induced expression of *HSPA1A*, we treated lamin-knockdown cells with 100 µM $CdSO_4$ for 2 h, followed by qRT-PCR analyses of *HSPA1A* transcript levels (Fig. 4A; Fig. S4C–E). Interestingly, lamin depletion did not affect $CdSO_4$-induced upregulation of *HSPA1A* expression (Fig. 4C). This contrasts with a specific involvement of lamins in the repression of *HSPA1A* expression upon heat shock (Fig. 4B), further underscoring the role of lamins in specifically modulating the heat-shock response.

Lamin A/C is required for heat-shock-induced movement of the Hsp70 gene locus

The Hsp70 gene locus is in close proximity to the nuclear speckles and shows enhanced contact with nuclear speckles upon heat shock, which further enhances transcriptional upregulation (Khanna et al., 2014; Kim et al., 2020). Furthermore, increase in the contact of Hsp70 gene locus with nuclear speckles is significantly higher when cells are exposed to heat shock as compared to what is observed during metal ion stress (Hu et al., 2010). Since lamin depletion attenuates heat-shock-induced upregulation of *HSPA1A* (Fig. 4B,C), we examined whether lamin depletion also impacts heat-shock-induced repositioning of the Hsp70 gene locus. We subjected lamin-knockdown cells to heat shock at 42°C for 60 min, followed by sequential immunostaining and fluorescence *in situ* hybridization (immuno-3D FISH). We performed immunostaining for lamin B1 and SC35, followed by FISH using a fluorescently labeled probe for the Hsp70 gene locus (Fig. 4D,E; Fig. S3I–K). Visualization of lamin B1, SC35 and the Hsp70 gene locus together enabled measurement of the shortest distance to Hsp70 gene loci from both the nuclear lamina (which marks the nuclear envelope) and the nuclear speckles.

Hsp70 gene loci showed a significant movement toward the nuclear interior upon heat shock in lamin B1- and B2-depleted cells, as in control cells (siLacZ) (Fig. 4E, white arrows, F). Remarkably, lamin A/C knockdown significantly curtailed the movement of Hsp70 gene loci toward the nuclear interior upon heat shock (Fig. 4E, white arrows, F). Hsp70 gene loci are in close proximity to SC35 speckles (siLacZ at 37°C) (Fig. 4G). While, Hsp70 gene loci moved closer to the speckles upon heat shock (Fig. 4E,G), lamin depletion did not show any change in the localization of Hsp70 gene loci with respect to SC35 speckles upon heat shock. Of note, Hsp70 gene loci moved closer to the speckles upon lamin B2 depletion at 37°C (Fig. 4G).

The Hsp70 gene locus did not reposition either with respect to the nuclear lamina or the nuclear speckles upon $CdSO_4$ treatment (100 µM $CdSO_4$ for 2 h) (Fig. S4F–I). This suggests that enhanced contact with nuclear speckles and repositioning away from the nuclear periphery are specific features of heat-shock-induced expression of the Hsp70 gene locus. Taken together, these analyses reveal that lamins are potentially required for enhanced contact between the Hsp70 gene locus and SC35 speckles upon heat shock, whereas lamin A/C uniquely regulates the heat-shock-mediated spatial repositioning of the Hsp70 gene locus with respect to the nuclear lamina.

Since nuclear speckles induce heat-shock-mediated expression of Hsp70 gene locus, we determined whether lamin depletion impacts the size and spatial distribution of the SC35 speckles (Fig. S5A). Imaging and analyses of SC35 speckles revealed that the speckle volume marginally decreases in siLamin B2 cells at 37°C, while lamin knockdown significantly decreases speckle volumes upon heat shock (Fig. S5B). Speckle volumes remained unchanged in control cells (siLacZ) before or after heat shock (Fig. S5B). Of note, number of SC35 speckles show a marginal increase per nucleus upon lamin B1 depletion (Fig. S5D).

We examined the spatial distribution of the SC35 speckles by measuring the shortest distance of each individual speckle from the nuclear lamina (Fig. S5C). Upon heat shock, SC35 speckles repositioned closer toward the nuclear periphery in control cells (siLacZ, 42°C) (Fig. S5C). Furthermore, depletion of either of the lamins relocalized nuclear speckles toward the nuclear periphery, even in the absence of heat shock (Fig. S5C). Of note, lamin A/C depletion showed a similar organization of SC35 speckles as control cells upon heat shock (Fig. S5C). Notwithstanding a minor decrease in nuclear area upon lamin A/C or B2 depletion (Fig. S6E,F), nuclear lamins modulate the topology and spatial positioning of the SC35 nuclear speckles in the interphase nucleus.

Lamin A overexpression rescues the expression and spatial repositioning of the Hsp70 gene locus upon heat shock

We examined the specificity of lamin A in regulating the dynamics and function of the Hsp70 gene locus by overexpressing GFP–lamin A (siRNA resistant) in cells depleted of endogenous lamin A/C and examining the (1) expression and (2) spatial localization of the Hsp70 gene locus upon heat shock (Fig. 5A,B). While lamin A/C depletion attenuates heat-shock-mediated upregulation of *HSPA1A,* overexpression of GFP–lamin A (siRNA resistant) rescued *HSPA1A* transcript levels upon heat shock (Fig. 5B; Fig. S6D).

We performed immuno-3D FISH for the Hsp70 gene locus with (1) lamin B1 (marker of the nuclear envelope) and (2) GFP (marker of lamin A-overexpressing cells), in endogenous lamin A/C-depleted cells overexpressing GFP–lamin A (siRNA resistant) upon heat shock (Fig. 5C,D). Interestingly, GFP–lamin A overexpression in otherwise lamin A/C-depleted cells, rescued and re-localized Hsp70 gene loci toward the nuclear interior upon heat shock (Fig. 5D).

We next sought to distinguish whether the nuclear envelope-associated lamin A or the nucleoplasmic pool of lamin A

Journal of Cell Science (2020) 133, jcs236265. doi:10.1242/jcs.236265

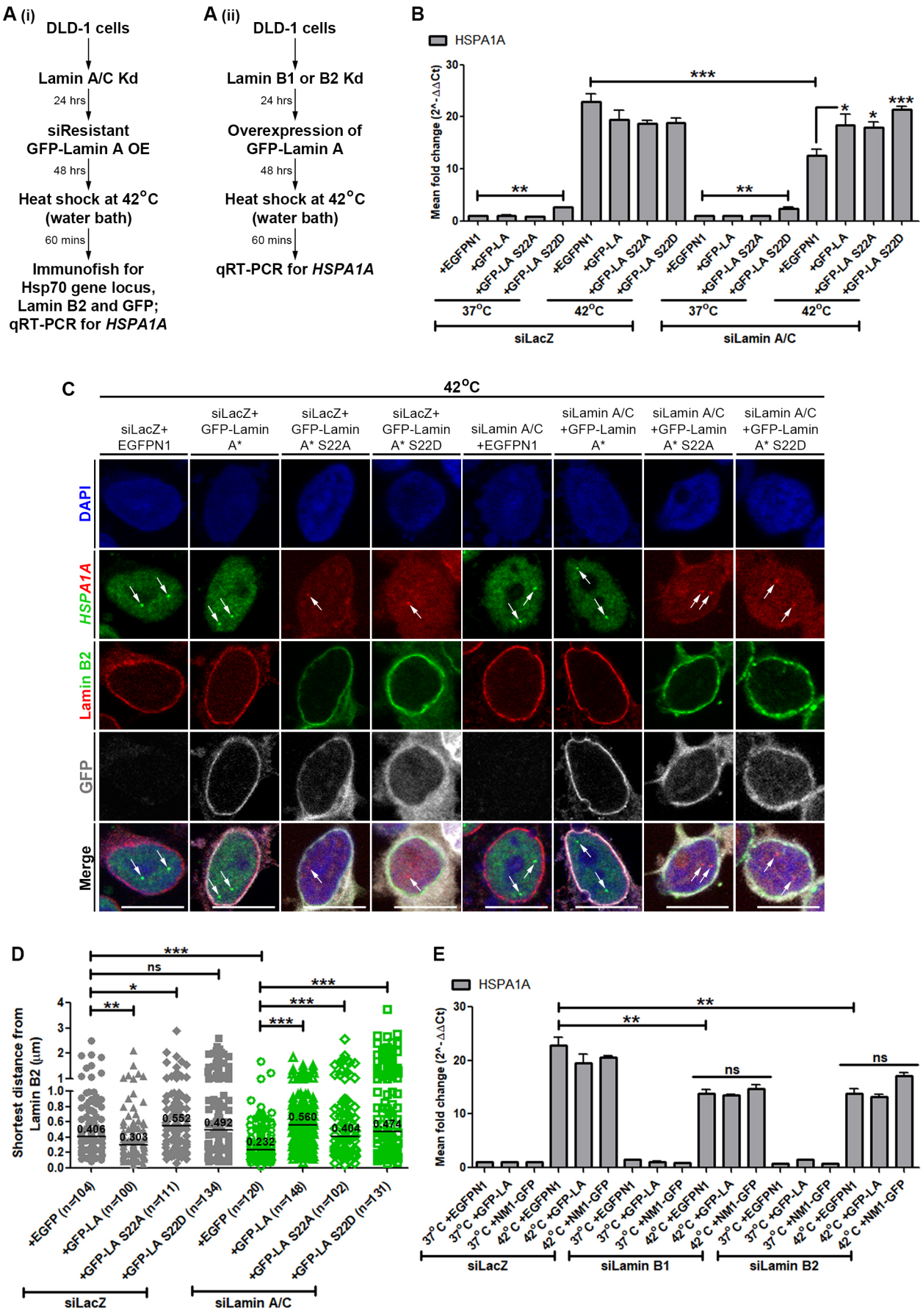

Fig. 5. See next page for legend.

Fig. 5. Overexpression of GFP-lamin A WT, S22A or S22D rescues the expression and spatial dynamics of the Hsp70 gene locus. (Ai,Aii) Experimental scheme. (B) Measurement of mean±s.e.m. *HSPA1A* transcript levels using qRT-PCR in siLacZ and siLamin A/C cells overexpressing (OE) EGFP-N1, siRNA-resistant GFP-lamin A (LA) WT, S22A or S22D. Expression was normalized to the internal control (GAPDH) and then to the siLacZ+EGFP-N1 37°C control. Combined data are from two independent biological replicates (n=6). *P<0.05; **P<0.01; ***P<0.0001 (Student's t-test). (C) Representative mid-optical sections from confocal z-stacks showing lamin B2 and GFP immunostaining, and 3D-FISH for the Hsp70 gene locus (*HSPA1A*) in siLacZ and siLamin A/C cells, overexpressing EGFP-N1, siRNA-resistant GFP-lamin A (GFP-lamin A*) WT, S22A or S22D upon heat shock at 42°C for 60 min (controls: siRNA-treated cells at 37°C, Fig. S6A–D). White arrows highlight specific hybridization of BAC DNA probe showing two copies of the Hsp70 gene locus. Scale bars: 10 µm. (D) Dot scatter plot and median showing the shortest distance (in µm) of the Hsp70 loci from lamin B2 staining in control cells treated with siLacZ and overexpressing EGFP-N1, and siRNA-resistant GFP–lamin A, S22A and S22D, and siLamin A/C cells overexpressing EGFP-N1, and siRNA-resistant GFP-lamin A, S22A and S22D, upon heat shock at 42°C for 60 min (controls: siRNA-treated cells at 37°C, Fig. S4A–C). Data from two independent biological replicates; the number of nuclei analyzed is given on the figure (n). *P<0.05; **P<0.01; *** P<0.0001; ns, not significant (Mann–Whitney test). (E) Measurement of mean±s.e.m. *HSPA1A* transcript levels using qRT-PCR in siLacZ, siLamin B1 and siLamin B2 cells overexpressing EGFP-N1, GFP–lamin A WT or NM1–GFP. Expression was normalized to internal control (GAPDH) and then to siLacZ+EGFP-N1 37°C control. Combined data from two independent biological replicates (n=6). **P<0.01; ns, not significant (Student's t-test).

differentially modulates expression and dynamics of Hsp70 gene locus. We created independent point mutations in lamin A, first a S22D phosphomimetic mutant which shows enhanced localization in the nucleoplasm, and second a S22A phosphodeficient mutant of lamin A, which is predominantly localized at the nuclear envelope (Kochin et al., 2014). We examined the expression and dynamics of the Hsp70 gene locus upon overexpressing (1) siRNA-resistant GFP-lamin A S22A and (2) S22D in lamin A/C-depleted cells (Fig. 5A–D). Interestingly, both mutants rescue the expression and dynamics of the Hsp70 gene locus in a manner that is comparable to the rescue seen with wild type (WT) lamin A (Fig. 5B,D). In summary, nucleoplasmic or nuclear envelope-associated lamin A does not show significant differences in regulating heat-shock-mediated expression and dynamics of the Hsp70 gene locus. Furthermore, overexpression of either WT lamin A or mutant lamins (S22A or S22D) does not affect the spatial positions of Hsp70 gene locus at 37°C (Fig. S6A–D), while overexpression of lamin A S22D upregulates *HSPA1A* expression by ∼2.5 fold in the absence of heat shock (Fig. 5B). Taken together, these results strongly implicate lamin A/C in regulating the movement of the Hsp70 gene locus toward the nuclear interior upon heat shock.

We tested whether lamin A overexpression rescues the otherwise attenuated expression of *HSPA1A* in B-type lamin-depleted cells upon heat shock (Fig. 5E). Overexpression of GFP–lamin A in B-type lamin-depleted cells (siLamin B1 and siLamin B2) does not rescue the attenuated expression of *HSPA1A* upon heat shock (Fig. 5E), suggesting mutually exclusive functions of A and B-type lamins in regulating Hsp70 gene expression.

Lamin A/C modulates Hsp70 gene loci movement potentially via NM1

Myosin 1c isoform B, known as nuclear myosin I (NM1), localizes in the nucleus and regulates long-range chromatin dynamics in the interphase nucleus (Chuang et al., 2006; Hofmann et al., 2006; Kulashreshtha et al., 2016; Pestic-Dragovich et al., 2000). NM1 interacts with emerin, which is also a direct interactor of lamin A/C (Holaska and Wilson, 2007; Lee et al., 2001). However, the functional significance of this interaction is unclear in the context of chromatin dynamics, during heat shock. The lamin A–emerin–NM1 complex, in conjunction with nuclear actin, is implicated in modulating chromatin dynamics (Mehta et al., 2008; Ranade et al., 2019). Considering that NM1 is a nuclear motor protein and interacts with actin that further modulates Hsp70 gene loci dynamics (Khanna et al., 2014), we addressed the mechanistic underpinnings of the heat-shock response, by examining the effect of heat shock on the lamin A–emerin–NM1 sub-complex. Interestingly, co-immunoprecipitation assays revealed an enhanced interaction between NM1 and emerin upon heat shock at 42°C (Fig. 6A, red asterisk), which was restored to basal levels upon recovery at 37°C (Fig. 6A,B). We showed that lamin A/C is required for maintaining the NM1–emerin interaction and for partitioning NM1 between the cytoplasm and the nucleus (Ranade et al., 2019). We therefore examined the subcellular localization of NM1 upon heat shock, and lamin depletion. NM1 is localized as punctate foci at the plasma membrane and in the nucleoplasm (Fig. 6C). Consistent with previous results, intranuclear NM1 foci increase upon lamin A/C depletion at 37°C (Fig. 6C,D) (Ranade et al., 2019). Heat shock caused a significant increase in numbers of intranuclear NM1 foci upon lamin B1 or B2 knockdown or in control cells (siLacZ), suggesting that lamin B1 or B2 depletion does not affect the response of NM1 to heat shock (Fig. 6C,D). In contrast, lamin A/C knockdown did not cause an increase in NM1 intranuclear foci upon heat shock (Fig. 6C,D). Taken together, this further underscores a specific role of lamin A/C as a modulator of NM1 localization in the nucleus.

To further determine whether NM1 is a downstream target of lamin A/C, we independently overexpressed GFP–lamin A in a background of NM1 depletion and conversely overexpressed NM1–GFP in a lamin A/C depletion background. We exposed these cells to heat shock at 42°C for 60 min, and analyzed transcript levels of *HSPA1A* using qRT-PCR (Fig. 6F,G). Interestingly, siNM1 cells showed an ∼2-fold decrease in *HSPA1A* transcript levels at 42°C whereas control cells (siLacZ) showed an ∼20-fold upregulation of *HSPA1A* expression upon heat shock (Fig. 6F, Fig. S8A,B), suggesting that NM1 is indeed required for heat-shock-induced transcriptional upregulation of *HSPA1A*. Although overexpression of NM1–GFP in lamin A/C-knockdown cells partially rescued transcript levels of *HSPA1A* upon heat shock (Fig. 6G), the overexpression of GFP–lamin A in NM1 knockdown cells was unable to rescue *HSPA1A* expression (Fig. 6F). These results suggest that NM1 functions downstream of lamin A/C. Interestingly, NM1–GFP overexpression in B-type lamin-depleted cells (siLamin B1 or siLamin B2) did not rescue the otherwise attenuated expression of *HSPA1A,* reiterating the distinct roles of A and B-type lamins in regulating *HSPA1A* expression (Fig. 5E). In summary, lamin A/C regulates the spatial dynamics and expression levels of the Hsp70 gene locus during heat shock by modulating the localization and, potentially, the activity of NM1 in the interphase nucleus.

NM1 depletion abrogates heat-shock-induced movement of the Hsp70 gene locus

We next investigated the underlying mechanistic role of NM1 during heat shock by examining the induction of *HSPA1A* expression and analyzing the spatial positions of the Hsp70 gene loci upon NM1 inhibition and knockdown (Chon et al., 2001; Steinberg and McIntosh, 1998). Cells treated with 1 mM 2,3 butanediol-monoxime (BDM), an NM1 inhibitor, for 90 min, or NM1 knockdown showed a significant decrease in NM1 levels

Journal of Cell Science (2020) 133, jcs236265. doi:10.1242/jcs.236265

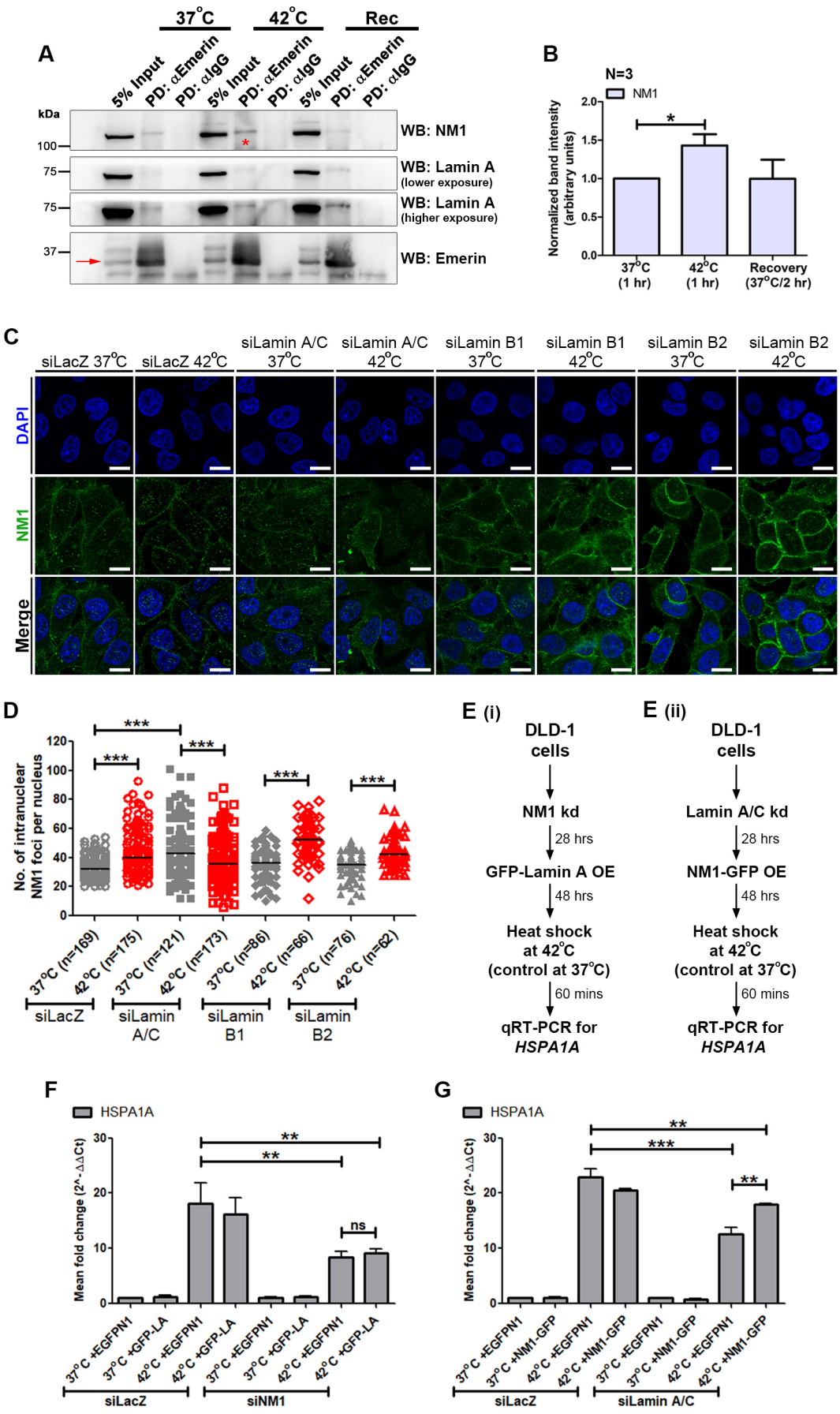

Fig. 6. See next page for legend.

Journal of Cell Science

Fig. 6. Lamin A/C is required for heat-shock-induced increase in NM1 intranuclear foci. (A) Representative co-immunoprecipitation (PD, pulldown) using anti-emerin antibody (red arrow), probed for NM1 and lamin A in control cells (37°C), cells subjected to heat shock at 42°C for 60 min and upon recovery for 2 h. The asterisk highlights the presence of emerin in the PD. (B) Densitometric quantification of mean±s.e.m. band intensities for NM1 in emerin pulldown upon heat shock at 42°C (control cells at 37°C) and upon recovery. Both emerin and NM1 levels were normalized to their respective inputs, and the extent of NM1 pulled down with emerin was further normalized to total emerin pulldown. Data from three independent biological replicates. **P*<0.05 (Student's *t*-test). (C) Representative mid-optical section images from confocal *z*-stacks showing immunostaining of NM1 and emerin in lamin-knockdown cells upon heat shock at 42°C for 60 min (controls, 37°C). Immunostaining shows both cytoplasmic and intranuclear fractions of NM1. (D) Dot scatter plot and median of intranuclear NM1 foci numbers in lamin-knockdown cells exposed to heat shock. Data from two (siLamin B1 and B2) and three (siLacZ and siLamin A/C) independent biological replicates. ****P*<0.0001 (Mann–Whitney test). (Ei-Eii) Experimental scheme. (F) Measurement of mean±s.e.m. *HSPA1A* transcript levels using qRT-PCR in siNM1 cells overexpressing EGFP-N1 or GFP–lamin A WT. Expression was normalized to the internal control (GAPDH) and then to the siLacZ+EGFP-N1 37°C control. (G) Measurement of mean±s.e.m. *HSPA1A* transcript levels using qRT-PCR in siLamin A/C cells overexpressing EGFP-N1 or NM1–GFP. Expression was normalized to the internal control (GAPDH) and then to the siLacZ+EGFP-N1 37°C control. Combined data in F and G are from two independent biological replicates each (*n*=6 each). ***P*<0.01, ****P*<0.0001; ns, not significant (Student's *t*-test). Scale bars: 10 µm.

(Figs S7B–D, S8A,B). Interestingly, both NM1 inhibition or depletion attenuated *HSPA1A* expression levels to a similar extent as lamin A/C knockdown alone (Fig. 7A–C). NM1 inhibition in lamin A/C knockdown cells further decreased *HSPA1A* transcript levels at 42°C (Fig. 7B). However, co-depletion of lamin A/C and NM1 did not show an additive repression of *HSPA1A*, suggesting that inactive NM1 further contributes to the transcriptional repression of Hsp70 gene locus (Fig. 7C).

We asked whether NM1 modulates the spatial positions of the Hsp70 gene loci by performing immuno-3D FISH of the Hsp70 gene locus with regard to the location of the lamin B1 (nuclear envelope) and SC35 nuclear speckles upon NM1 loss (Fig. 7D,E). Interestingly, NM1 inhibition or knockdown abrogated the movement of the Hsp70 gene locus away from the nuclear envelope upon heat shock (Fig. 7E,F,H). While the Hsp70 gene locus was in close proximity to the SC35 speckles (Fig. 7G,I), NM1 inhibition upon heat shock or NM1 knockdown (at 37°C and 42°C) resulted in a marginal separation between the Hsp70 gene loci and SC35 speckles (Fig. 7G,I). These results underscore the importance of NM1 and its activity in regulating the expression and spatial positioning of the Hsp70 gene locus upon heat shock.

We examined the impact of NM1 depletion on the size and spatial distribution of the SC35 speckles (Fig. S5A). Interestingly, loss of NM1 (1) causes a decrease in the volume of SC35 speckles and (2) relocalization of the speckles toward the nuclear interior at both 37°C and 42°C (Fig. S5C). This reorganization of SC35 speckles correlates with the increased distance between Hsp70 gene locus and SC35 in siNM1 cells, wherein the Hsp70 locus is positioned closer to the nuclear periphery, while the speckles are redistributed toward the nuclear interior (Fig. 7H–I; Fig. S5C). In summary, these results highlight an intricate regulatory cross talk between lamin A/C and NM1 in mediating the spatial organization and function of the Hsp70 gene locus and its association with nuclear speckles in the interphase nucleus.

DISCUSSION

Heat-shock signaling involves a physiologically important regulatory network of molecular chaperones that are activated in response to an aggregation of misfolded proteins upon thermal stress (Richter et al., 2010). This network is highly important for the immediate activation of the heat-shock response (Velichko et al., 2013). The Hsp70 gene locus is transcriptionally activated upon heat shock and shows enhanced contacts with nuclear speckles, which amplifies gene expression (Khanna et al., 2014; Kim et al., 2020). Here, we show that lamin A/C regulates the spatial positioning of the Hsp70 gene locus and its expression upon heat shock via the nuclear motor protein NM1.

Lamins maintain nuclear structure and function, and have key roles in DNA replication, transcription, positioning of chromosome territories and regulation of gene expression among others (Butin-Israeli et al., 2015; Dechat et al., 2008; Ghosh et al., 2015; Gibbs-Seymour et al., 2015; Ranade et al., 2017; Shumaker et al., 2008; Singh et al., 2013). Lamins regulate RNA Pol II-mediated transcription by potentially functioning as docking sites for the polymerase (Heessen and Fornerod, 2007; Spann et al., 2002). Lamins directly interact with chromatin via lamina-associated domains (LADs) – regions of chromatin that are enriched in repressive histone marks such as H3K9me2, and are devoid of signatures of active transcription such as RNA Pol II and histone modifications such as H3K4me3 (Guelen et al., 2008; Meuleman et al., 2013). The spatial organization of a gene locus in the interphase nucleus largely correlates with its expression levels (Khanna et al., 2014; Meaburn et al., 2009, 2016; Volpi et al., 2000; Williams et al., 2002). For instance, tethering a reporter gene to the nuclear lamina using a GFP-LacI-ΔEMD and lacO system represses gene expression (Reddy et al., 2008). Lamina-associating sequences (LASs) tether with the nuclear lamina and recruit repressors such as cKrox and HDAC3 (Zullo et al., 2012). Tethering chromatin to the inner nuclear membrane via the LacI–lacO system represses a subset of genes, owing to the activity of class I/II HDACs localized near the nuclear envelope (Finlan et al., 2008). Interestingly, gene loci targeted to the nuclear envelope can also be transcriptionally active (Kumaran and Spector, 2008). As lamins are regulators of nuclear mechanotransduction (Dahl et al., 2008; Hale et al., 2008; Lammerding et al., 2005; Osmanagic-Myers et al., 2015), lamins might potentially perceive and relay effects of thermal stress. Lamin B is upregulated upon heat shock in U-1 melanoma and HeLa cells, but is downregulated in response to heat shock in CHO cells (Dynlacht et al., 1999; Falloon and Dynlacht, 2002; Zhu et al., 1999). The nuclear envelope proteins emerin and lamin B1 are downregulated during recovery from heat shock in HeLa S3 cells (Haddad and Paulin-Levasseur, 2008). Lamins therefore also show diverse responses during heat shock, in a cell-type-specific manner.

Lamin A/C modulates nuclear import of Hsp70

Lamin A (~1.2 fold) and B1 (~2 fold) are upregulated to variable extents in response to heat shock (Figs 1D,E, 2C). Of note, lamin A/C, but not B-type lamins, modulate the import of Hsp70 into the nucleus upon heat shock (Fig. 3D). The import carrier Hikeshi, is required for the nuclear import of Hsp70 (Imamoto and Kose, 2012). Lamin A/C depletion may impact nuclear translocation of Hsp70 or impact Hikeshi activity. Overexpression of progerin (a mutant form of lamin A associated with accelerated ageing or progeria) shows variable effects on nuclear import. Busch et al. showed decreased nuclear import of a reporter plasmid (GFP-NLS) upon overexpression of progerin in HeLa cells, potentially due to mislocalization of the nucleoporin Nup153. However, Ferri et al. found that nucleo-cytoplasmic transport is unaffected under similar experimental conditions in U2OS cells (Busch et al., 2009; Ferri et al., 2017). HGPS patient fibroblasts and ESC-derived

Journal of Cell Science (2020) 133, jcs236265. doi:10.1242/jcs.236265

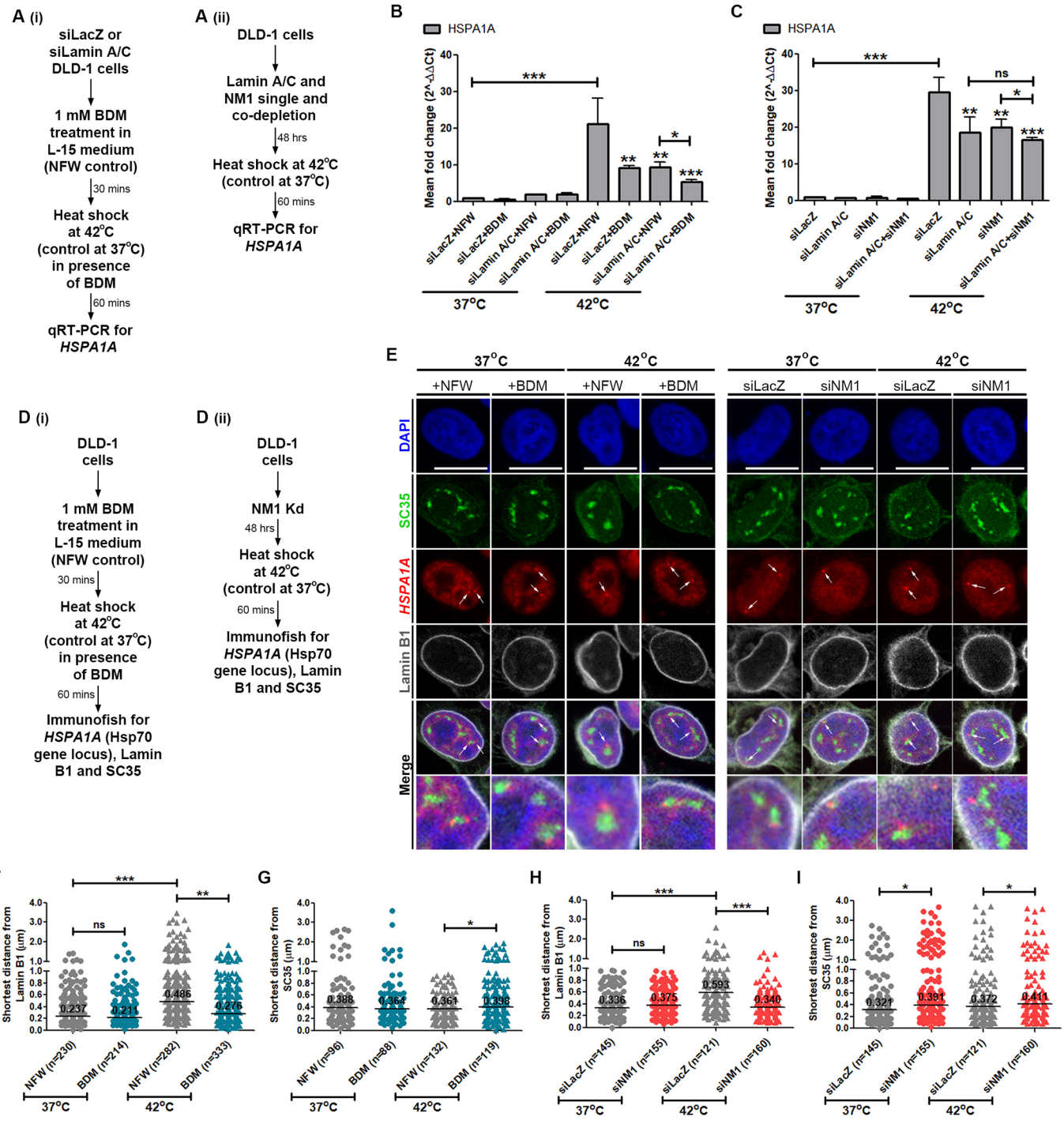

Fig. 7. NM1 inhibition or knockdown attenuates heat-shock-induced upregulation of *HSPA1A* and spatial repositioning of Hsp70 gene locus. (Ai,Aii) Experimental scheme. (B) Measurement of mean±s.e.m. *HSPA1A* transcript levels using qRT-PCR in siLacZ and siLamin A/C cells, subjected to NM1 inhibition using BDM and heat shock at 42°C (control: NFW). Expression was normalized to the internal control (GAPDH) and then to siLacZ 37°C+NFW. (C) Measurement of mean±s.e.m. *HSPA1A* transcript levels using qRT-PCR in siLacZ cells and cells with single and co-depletion of lamin A/C and NM1, subjected to heat shock at 42°C (control: NFW). Expression was normalized to the internal control (GAPDH) and then to siLacZ 37°C. Combined data in B and C are from two independent biological replicates (n=6 each). *P<0.05; **P<0.001; ***P<0.0001; ns, not significant (Student's t-test). (Di,Dii) Experimental scheme. (E) Representative mid-optical sections from confocal z-stacks showing SC35 and lamin B1 immunostaining, and 3D-FISH for the Hsp70 gene locus (*HSPA1A*), in cells treated with BDM or siRNA against NM1, subjected to heat shock at 42°C. White arrows highlight specific hybridization of BAC DNA probe showing two copies of the Hsp70 gene locus. (F) Dot scatter plot and median showing the shortest distance (in µm) of the Hsp70 loci from lamin B1 staining in cells treated with BDM and subjected to heat shock at 42°C. Data from four independent biological replicates. (G) Dot scatter plot and median showing the shortest distance of the Hsp70 loci from SC35 speckles in cells treated with BDM and heat shock at 42°C. Data from two independent biological replicates. (H) Dot scatter plot and median showing the shortest distance of the Hsp70 loci from lamin B1 staining in siNM1 cells subjected to heat shock at 42°C. Data from two independent biological replicates. (I) Dot scatter plot and median showing the shortest distance of the Hsp70 loci from SC35 speckles in siNM1 upon heat shock at 42°C. Data from *two* independent biological replicates. In F–I, the number of nuclei analyzed is given on the figure (n). *P<0.05; **P<0.01; ***P<0.0001; ns, not significant (Mann–Whitney test). Scale bars: 10 µm.

Journal of Cell Science

Journal of Cell Science (2020) 133, jcs236265. doi:10.1242/jcs.236265

fibroblast-like cells (EDFCs) derived from lamin A/C- and B1-knockout mESCs show altered distribution of nuclear pore complexes (Goldman et al., 2004; Guo et al., 2014; Sullivan et al., 1999). A and B-type lamins show differential association with the nuclear pore complex proteins that may differentially impact cargo movement through the NPC (Xie et al., 2016). Therefore, understanding the mechanisms of lamin interaction with nuclear import factors or nucleoporins is essential for understanding the role of lamins in the heat-shock response pathway.

Differential regulation of *HSPA1A* transcription by nuclear lamins

Although the Hsp70 gene locus is located in close proximity to nuclear speckles, enhanced contact of Hsp70 gene locus with the speckles upon heat-shock results in its transcriptional upregulation (Jolly et al., 1999; Khanna et al., 2014; Kim et al., 2020). Furthermore, the *HSPA1A* promoter is essential since the artificial introduction of this promoter upstream of another gene, *MT2A*, induced its movement toward nuclear speckles coupled with its expression upon heat shock (Hu et al., 2010). Endogenous Hsp70 gene loci are in close proximity to SC35 speckles, and move further toward SC35 and away from the nuclear envelope upon heat shock, but not cadmium sulfate treatment (an independent inducer of Hsp70 gene locus activation) (Fig. 4F,G; Fig. S4F–I). Interestingly, we identified a requirement for nuclear lamins only in the heat-shock-induced upregulation of *HSPA1A* (Fig. 4B,C). Both metal ion stress and heat shock upregulate *HSPA1A* gene expression via the HSF1 pathway (Williams and Morimoto, 1990). This indicates that lamins regulate the heat-shock response downstream of HSF1. HSF1 binding at the *HSPA1A* gene promoter induces recruitment of the transcription machinery and actin-dependent movement of the gene locus toward nuclear speckles for enhanced transcription (Khanna et al., 2014; Kim et al., 2020). Examining the spatial positions of the Hsp70 gene loci revealed that, while lamin A/C knockdown abrogates heat-shock-induced movement of the Hsp70 gene locus away from the nuclear envelope (Fig. 4F), lamin depletion does not affect the proximity of the locus to SC35 speckles (Fig. 4G). This further correlates with the spatial redistribution of SC35 speckles toward the nuclear periphery upon lamin depletion (Fig. S5C). We surmise that while lamins are important regulators of SC35 speckle organization in the interphase nucleus, the impact of lamin A/C on Hsp70 gene locus potentially stems from its control of locus movement upon heat shock.

Lamin A/C and its direct interactor emerin, bind to and regulate actin polymerization (Holaska et al., 2004; Ondrej et al., 2008; Simon et al., 2010). Furthermore, emerin directly interacts with the nuclear motor protein NM1, which assists in chromatin dynamics and remodeling during transcription by RNA Pol I, II and III (Almuzzaini et al., 2015; Chuang et al., 2006; Hofmann et al., 2006; Holaska and Wilson, 2007; Mehta et al., 2008; Percipalle et al., 2006; Pestic-Dragovich et al., 2000). Lamin A/C is also required for the localization of emerin at the inner nuclear membrane (Vaughan et al., 2001). Interestingly, lamin A/C modulates levels of intranuclear NM1 foci upon heat shock (Fig. 6D), while inhibition or knockdown of NM1 attenuates *HSPA1A* expression upon heat shock, similar to what is seen upon lamin A/C knockdown alone (Fig. 7B,C). Additionally, NM1 inhibition and depletion abrogates heat-shock-induced movement of the Hsp70 gene locus toward the nuclear interior (Fig. 7F,H). NM1 knockdown repositions SC35 speckles toward the nuclear interior, as evidenced by a marginally increased separation between the Hsp70 gene loci and SC35 speckles in siNM1 cells, both in the presence and absence of heat shock (Fig. 7G,I). Therefore, NM1 is an important modulator of heat-shock-induced reorganization of the SC35 speckles and repositioning of the Hsp70 gene locus. We propose that lamin A/C loss perturbs nuclear localization of NM1 and its activity, potentially in an emerin-dependent manner (Fig. 8). Additionally, NM1 is bound near the promoters of a subset of heat-shock genes in mouse embryonic fibroblasts (MEFs) and also interacts with the WSTF–SNF2h chromatin-remodeling complex (Almuzzaini et al., 2015; Percipalle et al., 2006). Any alterations in NM1 localization or activity could further affect the remodeling activity of this complex, impeding appropriate transcriptional responses.

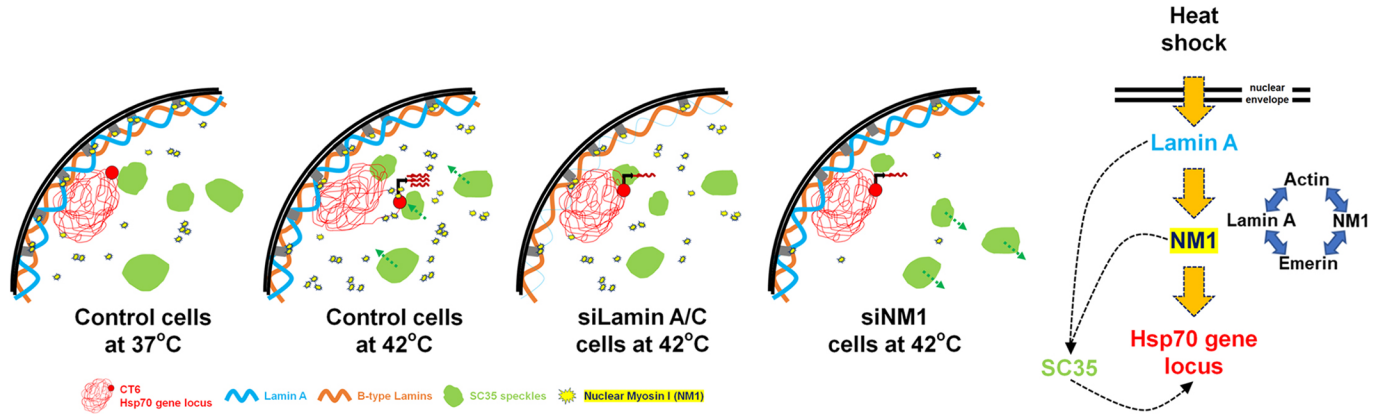

Fig. 8. Model depicting regulation of the Hsp70 gene locus by lamin A/C and NM1. The Hsp70 gene locus moves away from the nuclear envelope and shows enhanced contact with SC35 nuclear speckles upon heat shock, which further assists in increasing its expression (Hu et al., 2010; Khanna et al., 2014; Kim et al., 2020). Heat shock redistributes nuclear speckles toward the nuclear periphery. Depletion of lamin A/C, inhibition of NM1 activity or NM1 depletion, attenuates heat-shock-mediated induction of *HSPA1A* (a gene which is a part of the Hsp70 locus), by abrogating the movement of the gene locus toward the nuclear interior. Furthermore, depletion of lamin A/C repositions the SC35 speckles toward the nuclear periphery even in the absence of heat shock, but does not alter the proximity of the Hsp70 gene locus to the speckles. Interestingly, NM1 knockdown repositions the speckles toward the nuclear interior at both 37°C and 42°C, as reflected in the increased spatial separation between the Hsp70 gene locus and the speckles. We propose that loss of lamin A/C impairs (1) partitioning of the nuclear motor NM1, between the cytoplasm and the nucleus, (2) potentially NM1 activity and (3) the stability of the actin–emerin–NM1 subcomplex upon heat shock. Our results highlight a novel regulatory role for lamin A/C and NM1 in the modulation of the physiologically critical heat shock response pathway.

Journal of Cell Science (2020) 133, jcs236265. doi:10.1242/jcs.236265

Interestingly, while depletion of B-type lamins attenuates *HSPA1A* gene expression (Fig. 4B), it does not impact the movement of the Hsp70 gene locus toward the nuclear interior upon heat shock (Fig. 4F). We speculate that lamin B1 and B2 potentially recruit transcription factors such as NF-Y, NF-κB and CREB that are required for the upregulation of Hsp70 locus expression after it has contacted nuclear speckles (Erkina et al., 2010; Mahat et al., 2016; Sasi et al., 2014). Furthermore, B-type lamins also regulate the organization of the SC35 speckles in the nucleus (Fig. S5C). This suggests a regulatory role for lamins in modulating the association of the Hsp70 gene locus, with nuclear speckles and could potentially extend to other heat shock inducible and speckle associated gene loci as well. In summary, these results highlight an important role for lamins in regulating nuclear organization during heat shock and a novel regulatory partnership between lamin A/C and NM1 in the modulation of the expression and dynamics of the Hsp70 gene locus.

MATERIALS AND METHODS

Cell culture

DLD-1 colorectal adenocarcinoma cells were obtained from Thomas Ried (NCI, NIH, Bethesda, MD). DLD-1 cells were maintained in RPMI medium (Invitrogen, RPMI 1640, 11875-093) supplemented with 10% fetal bovine serum (FBS, Invitrogen, 6140-079 Carlsbad, CA) and the antibiotics penicillin (100 U/ml) and streptomycin (100 µg/ml, Invitrogen, 15070-063) at 37°C with 5% CO_2. DLD-1 cells were validated by karyotyping metaphase chromosome spreads, which showed that these cells maintain pseudodiploid chromosome numbers of ∼44–46. Cells were routinely tested and found to be free of mycoplasma contamination.

Heat shock induction in DLD-1 cells

The culture medium of cells was first changed from complete RPMI 1640 medium to Leibovitz L-15 medium (Gibco, 21083-027; pre-warmed to room temperature before use). Culture dishes (either 35 mm×10 mm dishes with 8 cm^2 area, or 6-well plates with 9.5 cm^2 area per well, Corning®) containing cells were sealed with parafilm and exposed to either 37°C (control) or 42°C (heat shock) in water baths (for required time points), pre-set at these temperatures for at least 30-45 min to maintain stable temperatures.

siRNA-mediated knockdown

Cells (∼0.2×10^6) were seeded overnight for transfection. The siRNA transfection mix was prepared using Lipofectamine RNAimax in reduced serum medium [Opti-MEM, Invitrogen Cat No. 31985-070] and incubated at RT for 30 min. The siRNA mix was added to cells in complete RPMI 1640 medium and knockdown was continued for 48 h after which cells were used for further assays. Details of siRNAs used are given in Table S1.

Cadmium sulfate treatment

Cells were first transferred to fresh complete RPMI 1640 medium, followed by the addition of cadmium sulfate solution (1 mM stock, prepared in nuclease-free water). An equal volume of nuclease free water was added to control cells. Cells were maintained at 37°C, in 5% CO_2 incubator for the 2 h duration of the treatment.

Overexpression of siRNA-resistant GFP–lamin A WT, S22A and S22D

The pEGFP-Lamin A construct was a kind gift from Kaushik Sengupta (SINP, Kolkata, India) and was converted into an siRNA-resistant WT sequences using the primers shown in Table S2. Point mutations were introduced in siRNA-resistant GFP–Lamin A WT to generate GFP–Lamin A S22A and S22D mutants. Cells (∼0.2×10^6) were seeded overnight for siRNA transfection. Transfection mix was prepared using Lipofectamine RNAimax in Opti-MEM containing 100 nM siRNA against LacZ and lamin A/C, and incubated at room temperature for 30 min. siRNA mix was then added to cells in complete RPMI 1640 medium and knockdown was continued for 24 h. After 24 h, cells were transfected with either EGFP-N1 (empty vector) or the siRNA-resistant GFP–Lamin A using Lipofectamine LTX and Plus reagent (Invitrogen, 15338100) for 48 h. After 48 h, heat-shock induction was carried out as described above.

Western blotting

Whole-cell extracts were prepared using the RIPA buffer (50 mM Tris-HCl pH 7.4, 150 mM NaCl, 0.1% SDS, 0.01% sodium azide, 0.5% sodium deoxycholate, 1 mM EDTA and 1% NP-40). Protein samples were denatured by boiling in 4× Laemmli buffer and resolved on a 10% acrylamide-bis acrylamide gel, followed by transfer to an activated PVDF membrane at a constant voltage of 90 V for 100 min. The membrane was blocked in 5% non-fat dried milk prepared in 1× Tris-buffered saline and 0.1% Tween 20 (1× TBST) for 1 h at room temperature. Primary antibody (details shown in Table S3) were prepared in 0.5% non-fat dried milk in 1× TBST and incubated overnight at 4°C or for 3 h at room temperature. Secondary antibody incubation was carried out for 1 h at room temperature. Blots were developed using chemiluminescent substrate (GE Healthcare; ECL Prime, 89168-782) and acquired at incremental exposures of 10 s under a chemiluminescence system LAS4000 (GE Healthcare).

Immunofluorescence assay

Cells growing on coverslips were washed briefly using 1× PBS (5 min, twice at room temperature) followed by fixation with 4% paraformaldehyde (PFA, Sigma, 158127) prepared in 1× PBS (pH 7.4) for 12 min, and permeabilization in 0.5% Triton X-100 (prepared in 1× PBS) for 10 min. Blocking was performed in 1% BSA (Sigma, A2153) solution (prepared in 1× PBS) for 30 min. Primary antibodies (Table S3) were diluted in 0.5% BSA and incubation with cells was carried out at room temperature for 90 min. Secondary antibodies were diluted in 1× PBS with 0.1% Triton X-100 (1× PBST) and incubation was carried out at room temperature for 60 min. Cells were counterstained with 0.05 µg/ml 4′,6-diamidino-2-phenylindole (DAPI) solution for 2 min at room temperature, washed in 1× PBS and mounted in Slowfade Gold Antifade (Invitrogen, S36937) and stored at 4°C until they were imaged.

Quantification of cells with nuclear translocation of Hsp70

Cells subjected to heat shock at 42°C (60 min) or control cells maintained at 37°C, were immunostained for Hsp70. DLD-1 cells at 37°C showed a faint Hsp70 staining in the cytoplasm, while upon heat shock, Hsp70 staining was pan-nuclear or localized distinctly in the nucleolus with increased fluorescence intensity. DAPI staining was used to demarcate the nuclear border, and cells that showed Hsp70 staining within the nucleus or nucleolus were scored positive for nuclear translocation of Hsp70 upon heat shock.

Quantification of nuclear area, volume and circularity

DAPI staining from the immunofluorescence assays was used to quantify the nuclear area, volume and circularity. Using ImageJ, the mid-optical section of the confocal *z*-stacks was selected. The DAPI channel was used for thresholding individual nuclei, and area and circularity was calculated. Nuclear volume was quantified across the entire 3D confocal stack using the Object Counter3D tool in ImageJ.

RNA isolation

Cells were harvested in Trizol reagent (Invitrogen, 15596018), collected in 1.5 ml microfuge tubes, vortexed briefly for 10 s and 100 µl chloroform per 500 µl Trizol was added. The mixture was vortexed for 10 s and incubated at room temperature for 10 min, followed by centrifugation (12,000 ***g*** for 15 min at 4°C). The aqueous phase was carefully collected in fresh 1.5 ml microfuge tubes. Equal volume of isopropanol was added, followed by vortexing for 15 secs and incubation at room temperature for 15 min. The samples were centrifuged again (12,000 ***g*** for 15 min at 4°C), and the RNA pellet was washed with 70% ethanol and dried at 37°C for 5–10 min. The RNA pellet was reconstituted in desired volume of nuclease-free water (NFW) and incubated at 37°C for 5 min and at 65°C for 5 min (without shaking). RNA was stored at −80°C till further use. RNA quantification was performed using a Nanodrop machine.

Journal of Cell Science (2020) 133, jcs236265. doi:10.1242/jcs.236265

Preparation of cDNA and qRT-PCR

cDNA was prepared using oligo(dT) primers and a Verso cDNA Synthesis Kit (Thermo Fisher Scientific, AB1453B). qRT-PCR was performed from cDNA templates using Kapa SyBr Fast qPCR Master Mix (2×) Universal (KK4602) and real-time PCR system (Bio-rad, CFX96) (Table S4). Transcript levels were determined after (first) normalization to the internal control GAPDH and further (second normalization) to the specific experimental control.

NM1 inhibition using BDM

Cells were transferred from complete RPMI 1640 medium to pre-warmed Leibovitz L-15 medium. BDM (Sigma, B0753-25G) was added at a final concentration of 1 mM (diluted from a 50 mM stock prepared in NFW; the control was an equal volume of NFW). Cells were incubated in a 37°C/5% CO_2 incubator for 30 min. Then, cells (+BDM) were subjected to heat shock at 42°C for 60 min, while cells maintained at 37°C for 60 min in water baths served as control.

Quantification of intranuclear NM1 foci

In cells immunostained for NM1, DAPI staining was used to demarcate the nuclear border in each individual cell using the Freehand selection of ImageJ. Switching to the fluorescence channel for NM1, the Find Maxima process was used to obtain a count of NM1 foci present inside the nuclear border. Noise tolerance was adjusted to exclude any ambiguous dim foci, and maintained for control and treatment sets. The plasma membrane fraction of NM1, which shows a continuous staining, is not considered in this analysis.

Immuno-3D FISH

Fixation

Cells post heat shock were immediately treated with CSK buffer (0.1 M NaCl, 0.3 M sucrose, 3 mM $MgCl_2$, 10 mM PIPES pH 7.4, 0.5% Triton X-100) for 6–7 min, followed by fixation using 4% PFA for 12 min at room temperature. After two washes in 1× PBS, cells were permeabilized in 0.5% Triton X-100 (in 1× PBS) for 15 min and incubated in 20% glycerol (in 1× PBS) for 45 min. This was followed by five or six freeze–thaw cycles in liquid nitrogen, and three washes in 1× PBS, 10 min in 0.1 M HCl, and two washes in 50% formamide 2× saline sodium citrate buffer, pH 7.4 (50% FA-2× SSC). Coverslips with fixed nuclei were stored at 4°C overnight (or until further use).

Immunofluorescence

The immunofluorescence protocol was followed as described above. After the final three washes of 1× PBST, coverslips were stored in 1× PBST for 30 min. Post-fixation was carried out in 4% PFA for 7 min and post-permeabilization in 0.5% Triton X-100 for 7 min, followed by two washes in 1× PBS and two washes in 50% FA-2 × SSC.

Preparation of BAC DNA probe for FISH

BAC clone RP11-92G8 (CHORI BACPAC Resources) for *HSPA1A* and *HSPA1L* was purified using the BAC isolation protocol optimized for 100 ml cultures (Villalobos et al., 2004). BAC DNA was labeled with aminoallyl-dUTP-Texas Red (Jena Bioscience, NU-803-TXR) or aminoallyl-dUTP-Rhodamine-12 (Jena Bioscience, NU-803-RHOX) using a Nick Translation Kit (Roche, 10976776001, following the kit protocol). The labeling reaction was carried out at 15°C for 2.5 h and terminated using 0.5 M EDTA, and DNA was precipitated using 3 M sodium acetate and ethanol. The labeled DNA pellet was resuspended in deionized formamide (pH 7.4) at 37°C, followed by addition of Master Mix containing dextran sulfate and 2× SSC. The probe was stored at −20°C until further use.

Hybridization

The *HSPA1A* probe was incubated at 37°C for 7 min with shaking at 750 rpm, followed by denaturation at 80°C for 5 min and quickly chilled on ice for 2 min. Pre-annealing was at 37°C for 45 min. The *HSPA1A* probe and immunostained nuclei were co-denatured at 80°C for 7 min, followed by hybridization in a moist sealed box at 37°C for 48 h.

Detection

Post hybridization, coverslips were washed in 50% FA-2X SSC (pH 7.4), three times for 5 min each time at 45°C, followed by 0.1× SSC washes (three times for 5 min each time) at 60°C. Coverslips were counterstained with DAPI for 2 min, washed in 2× SSC, mounted in Slowfade Gold Antifade and stored in 4°C until imaged.

Imaging

Confocal images for Immuno-3D FISH were acquired on a Zeiss LSM 710 confocal microscope (Carl Zeiss, Thornwood, NJ, USA) with 63× Plan-Apochromat 1.4 NA oil immersion objective, ZEN software and scan zoom of 1.5–2.0. *Z*-stacked images were acquired at 512×512 pixels per frame using a 8-bit pixel depth for each channel at a voxel size of 0.105 µm×0.105 µm×0.34 µm and line averaging set at 4, collected sequentially in a three-channel mode. Immunofluorescence imaging was performed using Leica TCS SP8 confocal laser scanning microscope with a 63× Plan-Apochromat 1.4 NA oil immersion objective, LAS X software and scan zoom of 1.0–1.5. *Z*-stacked images were acquired at 512×512 pixels per frame using a 8-bit pixel depth for each channel at a voxel size of 0.105 µm×0.105 µm×0.34 µm and frame averaging set to 4, collected sequentially in a three-channel mode.

Analyses

3D reconstruction of confocal stacks was performed using Huygens Professional software for DAPI (blue channel), *HSPA1A* (red or green channel), SC35 (green channel) and lamin A or B1 (far red channel). Lamin staining was set as envelope anchor. The center of mass (CM) for the thresholded *HSPA1A* locus signal was determined and the shortest distance between the anchor (lamin staining) and CM was computed. To compute the distance between the SC35 speckles and the Hsp70 loci, SC35 speckles were set as anchors and the shortest distance between the anchor surface (SC35) and CM of the gene loci was computed.

Co-immunoprecipitation of lamin A–emerin–NM1 complex

Cells post heat shock were lysed in co-immunoprecipitation buffer (50 mM Tris-HCl pH ∼8.0, 300 mM NaCl and 0.5% NP-40), kept on ice for 15 min and centrifuged at 14,000 rpm (∼20,000 ***g***) for 20 min at 4°C. Lysates were subjected to pre-clearing using 10 µl Dynabead–Protein G (Invitrogen, 10003D) for 45 min at 4°C on a rotary shaker at 6–7 rpm. Post pre-clearing, the protein concentration was estimated and 2 µg of either mouse anti-emerin (Santacruz, H-12 sc-25284) or normal mouse IgG (Millipore, 12-371) was added to 500 µg lysate. Antigen–antibody incubation was carried out at 4°C on a rotary shaker at 6–7 rpm overnight. 20 µl Dynabead–Protein G, previously blocked with 0.5 mg/ml BSA solution for 30 min at 4°C, were added to capture the antigen–antibody complex for 4 h at 4°C on a rotary shaker at 6–7 rpm. The beads containing the complex were washed 5–6 times with chilled co-immunoprecipitation buffer for 10 min at 4°C on a rotary shaker at 12–13 rpm. After the washes, antigen–antibody complex was eluted from the beads by boiling them at 95°C for 10 min in 2× Laemmli's buffer and SDS-PAGE followed by western blotting was carried out.

Statistical analyses

The band intensity (western blotting) and average fold change (qRT-PCR) values were compared using unpaired Student's *t*-test (two-tailed). Surface area, circularity, fluorescence intensities (IFA) and distances of Hsp70 gene loci from lamina or SC35 were compared using Mann–Whitney test. $P<0.05$ was considered statistically significant. Graphs were plotted using GraphPad Prism 5.0 and Microsoft Excel.

Acknowledgements

Authors are grateful to IISER-Pune for Microscopy facility and equipment support. We thank all members of the Chromosome Biology Lab for their critical comments. We thank members of Biology, IISER-Pune for generously sharing reagents. The GR2-GFP2-M9 construct was a kind gift from Ralph Kehlenbach (Department of Molecular Biology, Faculty of Medicine, GZMB, Georg-August-University, Gottingen, Germany).

Competing interests
The authors declare no competing or financial interests.

Author contributions
Conceptualization: R.P., M.J.N., K.S.; Methodology: R.P., M.J.N., K.S.; Software: R.P.; Validation: R.P., M.J.N.; Formal analysis: R.P., M.J.N.; Investigation: R.P., M.J.N., K.S.; Resources: R.P., K.S.; Writing - original draft: R.P., K.S.; Writing - review & editing: R.P., K.S.; Visualization: R.P., K.S.; Supervision: K.S.; Project administration: K.S.; Funding acquisition: K.S.

Funding
This work was supported by a Wellcome Trust-DBT India Alliance Intermediate Fellowship (grant no. 500164/Z/09/Z), Department of Biotechnology, Ministry of Science and Technology (DBT, grant no. BT/PR13956/GET/119/22/2015), Department of Science and Technology (DST) Science and Engineering Research Board (SERB, grant no. EMR/2016/003983) and Intramural funding from Indian Institute of Science Education and Research (IISER), Pune. R.P. received fellowship from CSIR, New Delhi while M.J.N. received student fellowships from Indian Institute of Science Education and Research Pune and DST-Inspire.

Supplementary information
Supplementary information available online at
http://jcs.biologists.org/lookup/doi/10.1242/jcs.236265.supplemental

References

Almuzzaini, B., Sarshad, A. A., Farrants, A.-K. Ö. and Percipalle, P. (2015). Nuclear myosin 1 contributes to a chromatin landscape compatible with RNA polymerase II transcription activation. *BMC Biol.* **13**, 35. doi:10.1186/s12915-015-0147-z

Baler, R., Dahl, G. and Voellmy, R. (1993). Activation of human heat shock genes is accompanied by oligomerization, modification, and rapid translocation of heat shock transcription factor HSF1. *Mol. Cell. Biol.* **13**, 2486-2496. doi:10.1128/MCB.13.4.2486

Bar, D. Z., Davidovich, M., Lamm, A. T., Zer, H., Wilson, K. L. and Gruenbaum, Y. (2014). BAF-1 mobility is regulated by environmental stresses. *Mol. Biol. Cell* **25**, 1127-1136. doi:10.1091/mbc.e13-08-0477

Bridger, J. M., Kill, I. R., O'Farrell, M. and Hutchison, C. J. (1993). Internal lamin structures within G1 nuclei of human dermal fibroblasts. *J. Cell Sci.* **104**, 297-306.

Broers, J. L., Machiels, B. M., van Eys, G. J., Kuijpers, H. J., Manders, E. M., van Driel, R. and Ramaekers, F. C. (1999). Dynamics of the nuclear lamina as monitored by GFP-tagged A-type lamins. *J. Cell Sci.* **112**, 3463-3475.

Busch, A., Kiel, T., Heupel, W.-M., Wehnert, M. and Hübner, S. (2009). Nuclear protein import is reduced in cells expressing nuclear envelopathy-causing lamin A mutants. *Exp. Cell Res.* **315**, 2373-2385. doi:10.1016/j.yexcr.2009.05.003

Butin-Israeli, V., Adam, S. A., Jain, N., Otte, G. L., Neems, D., Wiesmüller, L., Berger, S. L. and Goldman, R. D. (2015). Role of lamin b1 in chromatin instability. *Mol. Cell. Biol.* **35**, 884-898. doi:10.1128/MCB.01145-14

Cesarini, E., Mozzetta, C., Marullo, F., Gregoretti, F., Gargiulo, A., Columbaro, M., Cortesi, A., Antonelli, L., Di Pelino, S., Squarzoni, S. et al. (2015). Lamin A/C sustains PcG protein architecture, maintaining transcriptional repression at target genes. *J. Cell Biol.* **211**, 533-551. doi:10.1083/jcb.201504035

Chon, K., Hwang, H.-S., Lee, J.-H. and Song, K. (2001). The myosin ATPase inhibitor 2,3-butanedione-2-monoxime disorganizes microtubules as well as F-actin in Saccharomyces cerevisiae. *Cell Biol. Toxicol.* **17**, 383-393. doi:10.1023/A:1013748500662

Chuang, C.-H., Carpenter, A. E., Fuchsova, B., Johnson, T., de Lanerolle, P. and Belmont, A. S. (2006). Long-range directional movement of an interphase chromosome site. *Curr. Biol.* **16**, 825-831. doi:10.1016/j.cub.2006.03.059

Dahl, K. N., Ribeiro, A. J. S. and Lammerding, J. (2008). Nuclear shape, mechanics, and mechanotransduction. *Circ. Res.* **102**, 1307-1318. doi:10.1161/CIRCRESAHA.108.173989

Daugaard, M., Rohde, M. and Jäättelä, M. (2007). The heat shock protein 70 family: highly homologous proteins with overlapping and distinct functions. *FEBS Lett.* **581**, 3702-3710. doi:10.1016/j.febslet.2007.05.039

Dechat, T., Pfleghaar, K., Sengupta, K., Shimi, T., Shumaker, D. K., Solimando, L. and Goldman, R. D. (2008). Nuclear lamins: major factors in the structural organization and function of the nucleus and chromatin. *Genes Dev.* **22**, 832-853. doi:10.1101/gad.1652708

Dechat, T., Adam, S. A., Taimen, P., Shimi, T. and Goldman, R. D. (2010). Nuclear lamins. *Cold Spring Harb. Perspect. Biol.* **2**, a000547. doi:10.1101/cshperspect.a000547

Demirovic, D., de Toda, I. M., Nizard, C. and Rattan, S. I. S. (2014). Differential translocation of heat shock factor-1 after mild and severe stress to human skin fibroblasts undergoing aging in vitro. *J. Cell Commun. Signal.* **8**, 333-339. doi:10.1007/s12079-014-0244-8

Dynlacht, J. R., Story, M. D., Zhu, W.-G. and Danner, J. (1999). Lamin B is a prompt heat shock protein. *J. Cell. Physiol.* **178**, 28-34. doi:10.1002/(SICI)1097-4652(199901)178:1<28::AID-JCP4>3.0.CO;2-K

Erkina, T. Y., Zou, Y., Freeling, S., Vorobyev, V. I. and Erkine, A. M. (2010). Functional interplay between chromatin remodeling complexes RSC, SWI/SNF and ISWI in regulation of yeast heat shock genes. *Nucleic Acids Res.* **38**, 1441-1449. doi:10.1093/nar/gkp1130

Falloon, E. A. and Dynlacht, J. R. (2002). Reversible changes in the nuclear lamina induced by hyperthermia. *J. Cell. Biochem.* **86**, 451-460. doi:10.1002/jcb.10241

Ferri, G., Storti, B. and Bizzarri, R. (2017). Nucleocytoplasmic transport in cells with progerin-induced defective nuclear lamina. *Biophys. Chem.* **229**, 77-83. doi:10.1016/j.bpc.2017.06.003

Finlan, L. E., Sproul, D., Thomson, I., Boyle, S., Kerr, E., Perry, P., Ylstra, B., Chubb, J. R. and Bickmore, W. A. (2008). Recruitment to the nuclear periphery can alter expression of genes in human cells. *PLoS Genet.* **4**, e1000039. doi:10.1371/journal.pgen.1000039

Fricker, M., Hollinshead, M., White, N. and Vaux, D. (1997). Interphase nuclei of many mammalian cell types contain deep, dynamic, tubular membrane-bound invaginations of the nuclear envelope. *J. Cell Biol.* **136**, 531-544. doi:10.1083/jcb.136.3.531

Ghosh, S., Liu, B., Wang, Y., Hao, Q. and Zhou, Z. (2015). Lamin a is an endogenous SIRT6 activator and promotes SIRT6-mediated DNA repair. *Cell Rep.* **13**, 1396-1406. doi:10.1016/j.celrep.2015.10.006

Gibbs-Seymour, I., Markiewicz, E., Bekker-Jensen, S., Mailand, N. and Hutchison, C. J. (2015). Lamin A/C-dependent interaction with 53BP1 promotes cellular responses to DNA damage. *Aging Cell* **14**, 162-169. doi:10.1111/acel.12258

Goldman, R. D., Shumaker, D. K., Erdos, M. R., Eriksson, M., Goldman, A. E., Gordon, L. B., Gruenbaum, Y., Khuon, S., Mendez, M., Varga, R. et al. (2004). Accumulation of mutant lamin A causes progressive changes in nuclear architecture in Hutchinson-Gilford progeria syndrome. *Proc. Natl. Acad. Sci. USA* **101**, 8963-8968. doi:10.1073/pnas.0402943101

Guelen, L., Pagie, L., Brasset, E., Meuleman, W., Faza, M. B., Talhout, W., Eussen, B. H., de Klein, A., Wessels, L., de Laat, W. et al. (2008). Domain organization of human chromosomes revealed by mapping of nuclear lamina interactions. *Nature* **453**, 948-951. doi:10.1038/nature06947

Guo, Y., Kim, Y., Shimi, T., Goldman, R. D. and Zheng, Y. (2014). Concentration-dependent lamin assembly and its roles in the localization of other nuclear proteins. *Mol. Biol. Cell* **25**, 1287-1297. doi:10.1091/mbc.e13-11-0644

Haddad, N. and Paulin-Levasseur, M. (2008). Effects of heat shock on the distribution and expression levels of nuclear proteins in HeLa S3 cells. *J. Cell. Biochem.* **105**, 1485-1500. doi:10.1002/jcb.21968

Hale, C. M., Shrestha, A. L., Khatau, S. B., Stewart-Hutchinson, P. J., Hernandez, L., Stewart, C. L., Hodzic, D. and Wirtz, D. (2008). Dysfunctional connections between the nucleus and the actin and microtubule networks in laminopathic models. *Biophys. J.* **95**, 5462-5475. doi:10.1529/biophysj.108.139428

Heessen, S. and Fornerod, M. (2007). The inner nuclear envelope as a transcription factor resting place. *EMBO Rep.* **8**, 914-919. doi:10.1038/sj.embor.7401075

Hofmann, W. A., Johnson, T., Klapczynski, M., Fan, J.-L. and de Lanerolle, P. (2006). From transcription to transport: emerging roles for nuclear myosin I. *Biochem. Cell Biol.* **84**, 418-426. doi:10.1139/o06-069

Holaska, J. M. and Wilson, K. L. (2007). An emerin "proteome": purification of distinct emerin-containing complexes from HeLa cells suggests molecular basis for diverse roles including gene regulation, mRNA splicing, signaling, mechanosensing, and nuclear architecture. *Biochemistry* **46**, 8897-8908. doi:10.1021/bi602636m

Holaska, J. M., Kowalski, A. K. and Wilson, K. L. (2004). Emerin caps the pointed end of actin filaments: evidence for an actin cortical network at the nuclear inner membrane. *PLoS Biol.* **2**, E231. doi:10.1371/journal.pbio.0020231

Hozák, P., Sasseville, A. M., Raymond, Y. and Cook, P. R. (1995). Lamin proteins form an internal nucleoskeleton as well as a peripheral lamina in human cells. *J. Cell Sci.* **108**, 635-644.

Hu, Y., Plutz, M. and Belmont, A. S. (2010). Hsp70 gene association with nuclear speckles is Hsp70 promoter specific. *J. Cell Biol.* **191**, 711-719. doi:10.1083/jcb.201004041

Hutten, S., Wälde, S., Spillner, C., Hauber, J. and Kehlenbach, R. H. (2009). The nuclear pore component Nup358 promotes transportin-dependent nuclear import. *J. Cell Sci.* **122**, 1100-1110. doi:10.1242/jcs.040154

Imamoto, N. and Kose, S. (2012). Heat-shock stress activates a novel nuclear import pathway mediated by Hikeshi. *Nucleus* **3**, 422-428. doi:10.4161/nucl.21713

Jolly, C., Morimoto, R., Robert-Nicoud, M. and Vourc'h, C. (1997). HSF1 transcription factor concentrates in nuclear foci during heat shock: relationship with transcription sites. *J. Cell Sci.* **110**, 2935-2941.

Jolly, C., Vourc'h, C., Robert-Nicoud, M. and Morimoto, R. I. (1999). Intron-independent association of splicing factors with active genes. *J. Cell Biol.* **145**, 1133-1143. doi:10.1083/jcb.145.6.1133

Kantidze, O. L., Velichko, A. K. and Razin, S. V. (2015). Heat stress-induced transcriptional repression. *Biochemistry Mosc* **80**, 990-993. doi:10.1134/S0006297915080039

Khanna, N., Hu, Y. and Belmont, A. S. (2014). HSP70 transgene directed motion to nuclear speckles facilitates heat shock activation. *Curr. Biol.* **24**, 1138-1144. doi:10.1016/j.cub.2014.03.053

Kim, J., Venkata, N. C., Hernandez Gonzalez, G. A., Khanna, N. and Belmont, A. S. (2020). Gene expression amplification by nuclear speckle association. *J. Cell Biol.* **219**, e201904046. doi:10.1083/jcb.201904046

Kochin, V., Shimi, T., Torvaldson, E., Adam, S. A., Goldman, A., Pack, C.-G., Melo-Cardenas, J., Imanishi, S. Y., Goldman, R. D. and Eriksson, J. E. (2014). Interphase phosphorylation of lamin A. *J. Cell Sci.* **127**, 2683-2696. doi:10.1242/jcs.141820

Kose, S. and Imamoto, N. (2014). Nucleocytoplasmic transport under stress conditions and its role in HSP70 chaperone systems. *Biochim. Biophys. Acta* **1840**, 2953-2960. doi:10.1016/j.bbagen.2014.04.022

Kose, S., Furuta, M. and Imamoto, N. (2012). Hikeshi, a nuclear import carrier for Hsp70s, protects cells from heat shock-induced nuclear damage. *Cell* **149**, 578-589. doi:10.1016/j.cell.2012.02.058

Krachmarov, C. P. and Traub, P. (1993). Heat-induced morphological and biochemical changes in the nuclear lamina from Ehrlich ascites tumor cells in vivo. *J. Cell. Biochem.* **52**, 308-319. doi:10.1002/jcb.240520307

Kulashreshtha, M., Mehta, I. S., Kumar, P. and Rao, B. J. (2016). Chromosome territory relocation during DNA repair requires nuclear myosin 1 recruitment to chromatin mediated by ϒ-H2AX signaling. *Nucleic Acids Res.* **44**, 8272-8291. doi:10.1093/nar/gkw573

Kumaran, R. I. and Spector, D. L. (2008). A genetic locus targeted to the nuclear periphery in living cells maintains its transcriptional competence. *J. Cell Biol.* **180**, 51-65. doi:10.1083/jcb.200706060

Labade, A. S., Karmodiya, K. and Sengupta, K. (2016). HOXA repression is mediated by nucleoporin Nup93 assisted by its interactors Nup188 and Nup205. *Epigenetics Chromatin* **9**, 54. doi:10.1186/s13072-016-0106-0

Lammerding, J., Hsiao, J., Schulze, P. C., Kozlov, S., Stewart, C. L. and Lee, R. T. (2005). Abnormal nuclear shape and impaired mechanotransduction in emerin-deficient cells. *J. Cell Biol.* **170**, 781-791. doi:10.1083/jcb.200502148

Lee, K. K., Haraguchi, T., Lee, R. S., Koujin, T., Hiraoka, Y. and Wilson, K. L. (2001). Distinct functional domains in emerin bind lamin A and DNA-bridging protein BAF. *J. Cell Sci.* **114**, 4567-4573.

Mahat, D. B., Salamanca, H. H., Duarte, F. M., Danko, C. G. and Lis, J. T. (2016). Mammalian heat shock response and mechanisms underlying its genome-wide transcriptional regulation. *Mol. Cell* **62**, 63-78. doi:10.1016/j.molcel.2016.02.025

Marullo, F., Cesarini, E., Antonelli, L., Gregoretti, F., Oliva, G. and Lanzuolo, C. (2016). Nucleoplasmic Lamin A/C and Polycomb group of proteins: an evolutionarily conserved interplay. *Nucleus* **7**, 103-111. doi:10.1080/19491034.2016.1157675

Meaburn, K. J., Gudla, P. R., Khan, S., Lockett, S. J. and Misteli, T. (2009). Disease-specific gene repositioning in breast cancer. *J. Cell Biol.* **187**, 801-812. doi:10.1083/jcb.200909127

Meaburn, K. J., Agunloye, O., Devine, M., Leshner, M., Roloff, G. W., True, L. D. and Misteli, T. (2016). Tissue-of-origin-specific gene repositioning in breast and prostate cancer. *Histochem. Cell Biol.* **145**, 433-446. doi:10.1007/s00418-015-1401-8

Mehta, I. S., Elcock, L. S., Amira, M., Kill, I. R. and Bridger, J. M. (2008). Nuclear motors and nuclear structures containing A-type lamins and emerin: is there a functional link? *Biochem. Soc. Trans.* **36**, 1384-1388. doi:10.1042/BST0361384

Memon, S. B., Lian, L., Gadahi, J. A. and Genlin, W. (2016). Proteomic response of mouse pituitary gland under heat stress revealed active regulation of stress responsive proteins. *J. Therm. Biol.* **61**, 82-90. doi:10.1016/j.jtherbio.2016.08.010

Meuleman, W., Peric-Hupkes, D., Kind, J., Beaudry, J.-B., Pagie, L., Kellis, M., Reinders, M., Wessels, L. and van Steensel, B. (2013). Constitutive nuclear lamina-genome interactions are highly conserved and associated with A/T-rich sequence. *Genome Res.* **23**, 270-280. doi:10.1101/gr.141028.112

Moir, R. D., Yoon, M., Khuon, S. and Goldman, R. D. (2000). Nuclear lamins A and B1: different pathways of assembly during nuclear envelope formation in living cells. *J. Cell Biol.* **151**, 1155-1168. doi:10.1083/jcb.151.6.1155

Morimoto, R. I. (1998). Regulation of the heat shock transcriptional response: cross talk between a family of heat shock factors, molecular chaperones, and negative regulators. *Genes Dev.* **12**, 3788-3796. doi:10.1101/gad.12.24.3788

Ondrej, V., Lukásová, E., Krejcí, J., Matula, P. and Kozubek, S. (2008). Lamin A/C and polymeric actin in genome organization. *Mol. Cells* **26**, 356-361.

Osmanagic-Myers, S., Dechat, T. and Foisner, R. (2015). Lamins at the crossroads of mechanosignaling. *Genes Dev.* **29**, 225-237. doi:10.1101/gad.255968.114

Paradisi, M., McClintock, D., Boguslavsky, R. L., Pedicelli, C., Worman, H. J. and Djabali, K. (2005). Dermal fibroblasts in Hutchinson-Gilford progeria syndrome with the lamin A G608G mutation have dysmorphic nuclei and are hypersensitive to heat stress. *BMC Cell Biol.* **6**, 27. doi:10.1186/1471-2121-6-27

Pauli, D., Arrigo, A.-P. and Tissières, A. (1992). Heat shock response in Drosophila. *Experientia* **48**, 623-629. doi:10.1007/BF02118306

Percipalle, P., Fomproix, N., Cavellán, E., Voit, R., Reimer, G., Krüger, T., Thyberg, J., Scheer, U., Grummt, I. and Farrants, A.-K. O. (2006). The chromatin remodelling complex WSTF-SNF2h interacts with nuclear myosin 1 and has a role in RNA polymerase I transcription. *EMBO Rep.* **7**, 525-530. doi:10.1038/sj.embor.7400657

Pestic-Dragovich, L., Stojiljkovic, L., Philimonenko, A. A., Nowak, G., Ke, Y., Settlage, R. E., Shabanowitz, J., Hunt, D. F., Hozak, P. and de Lanerolle, P. (2000). A myosin I isoform in the nucleus. *Science* **290**, 337-341. doi:10.1126/science.290.5490.337

Pochukalina, G. N., Ilicheva, N. V., Podgornaya, O. I. and Voronin, A. P. (2016). Nucleolus-like body of mouse oocytes contains lamin A and B and TRF2 but not actin and topo II. *Mol. Cytogenet.* **9**, 50. doi:10.1186/s13039-016-0259-3

Polla, B. S., Stubbe, H., Kantengwa, S., Maridonneau-Parini, I. and Jacquier-Sarlin, M. R. (1995). Differential induction of stress proteins and functional effects of heat shock in human phagocytes. *Inflammation* **19**, 363-378. doi:10.1007/BF01534393

Prokocimer, M., Davidovich, M., Nissim-Rafinia, M., Wiesel-Motiuk, N., Bar, D. Z., Barkan, R., Meshorer, E. and Gruenbaum, Y. (2009). Nuclear lamins: key regulators of nuclear structure and activities. *J. Cell. Mol. Med.* **13**, 1059-1085. doi:10.1111/j.1582-4934.2008.00676.x

Ranade, D., Koul, S., Thompson, J., Prasad, K. B. and Sengupta, K. (2017). Chromosomal aneuploidies induced upon Lamin B2 depletion are mislocalized in the interphase nucleus. *Chromosoma* **126**, 223-244. doi:10.1007/s00412-016-0580-y

Ranade, D., Pradhan, R., Jayakrishnan, M., Hegde, S. and Sengupta, K. (2019). Lamin A/C and Emerin depletion impacts chromatin organization and dynamics in the interphase nucleus. *BMC Mol. Cell Biol.* **20**, 11. doi:10.1186/s12860-019-0192-5

Reddy, K. L., Zullo, J. M., Bertolino, E. and Singh, H. (2008). Transcriptional repression mediated by repositioning of genes to the nuclear lamina. *Nature* **452**, 243-247. doi:10.1038/nature06727

Richter, K., Haslbeck, M. and Buchner, J. (2010). The heat shock response: life on the verge of death. *Mol. Cell* **40**, 253-266. doi:10.1016/j.molcel.2010.10.006

Sarge, K. D., Murphy, S. P. and Morimoto, R. I. (1993). Activation of heat shock gene transcription by heat shock factor 1 involves oligomerization, acquisition of DNA-binding activity, and nuclear localization and can occur in the absence of stress. *Mol. Cell. Biol.* **13**, 1392-1407. doi:10.1128/MCB.13.3.1392

Sasi, B. K., Sonawane, P. J., Gupta, V., Sahu, B. S. and Mahapatra, N. R. (2014). Coordinated transcriptional regulation of Hspa1a gene by multiple transcription factors: crucial roles for HSF-1, NF-Y, NF-κB, and CREB. *J. Mol. Biol.* **426**, 116-135. doi:10.1016/j.jmb.2013.09.008

Shimi, T., Pfleghaar, K., Kojima, S., Pack, C.-G., Solovei, I., Goldman, A. E., Adam, S. A., Shumaker, D. K., Kinjo, M., Cremer, T. et al. (2008). The A- and B-type nuclear lamin networks: microdomains involved in chromatin organization and transcription. *Genes Dev.* **22**, 3409-3421. doi:10.1101/gad.1735208

Shumaker, D. K., Solimando, L., Sengupta, K., Shimi, T., Adam, S. A., Grunwald, A., Strelkov, S. V., Aebi, U., Cardoso, M. C. and Goldman, R. D. (2008). The highly conserved nuclear lamin Ig-fold binds to PCNA: its role in DNA replication. *J. Cell Biol.* **181**, 269-280. doi:10.1083/jcb.200708155

Simon, D. N., Zastrow, M. S. and Wilson, K. L. (2010). Direct actin binding to A- and B-type lamin tails and actin filament bundling by the lamin A tail. *Nucleus* **1**, 264-272. doi:10.4161/nucl.11799

Singh, M., Hunt, C. R., Pandita, R. K., Kumar, R., Yang, C.-R., Horikoshi, N., Bachoo, R., Serag, S., Story, M. D., Shay, J. W. et al. (2013). Lamin A/C depletion enhances DNA damage-induced stalled replication fork arrest. *Mol. Cell. Biol.* **33**, 1210-1222. doi:10.1128/MCB.01676-12

Smith, D. E. and Fisher, P. A. (1984). Identification, developmental regulation, and response to heat shock of two antigenically related forms of a major nuclear envelope protein in Drosophila embryos: application of an improved method for affinity purification of antibodies using polypeptides immobilized on nitrocellulose blots. *J. Cell Biol.* **99**, 20-28. doi:10.1083/jcb.99.1.20

Smith, D. E., Gruenbaum, Y., Berrios, M. and Fisher, P. A. (1987). Biosynthesis and interconversion of Drosophila nuclear lamin isoforms during normal growth and in response to heat shock. *J. Cell Biol.* **105**, 771-790. doi:10.1083/jcb.105.2.771

Snyers, L. and Schöfer, C. (2008). Lamina-associated polypeptide 2α forms complexes with heat shock proteins Hsp70 and Hsc70 in vivo. *Biochem. Biophys. Res. Commun.* **368**, 767-771. doi:10.1016/j.bbrc.2008.01.139

Spann, T. P., Goldman, A. E., Wang, C., Huang, S. and Goldman, R. D. (2002). Alteration of nuclear lamin organization inhibits RNA polymerase II-dependent transcription. *J. Cell Biol.* **156**, 603-608. doi:10.1083/jcb.200112047

Steinberg, G. and McIntosh, J. R. (1998). Effects of the myosin inhibitor 2,3-butanedione monoxime on the physiology of fission yeast. *Eur. J. Cell Biol.* **77**, 284-293. doi:10.1016/S0171-9335(98)80087-3

Stetler, R. A., Gan, Y., Zhang, W., Liou, A. K., Gao, Y., Cao, G. and Chen, J. (2010). Heat shock proteins: cellular and molecular mechanisms in the central nervous system. *Prog. Neurobiol.* **92**, 184-211. doi:10.1016/j.pneurobio.2010.05.002

Sullivan, T., Escalante-Alcalde, D., Bhatt, H., Anver, M., Bhat, N., Nagashima, K., Stewart, C. L. and Burke, B. (1999). Loss of A-type lamin expression compromises nuclear envelope integrity leading to muscular dystrophy. *J. Cell Biol.* **147**, 913-920. doi:10.1083/jcb.147.5.913

Tanguay, R. M. (1983). Genetic regulation during heat shock and function of heat-shock proteins: a review. *Can. J. Biochem. Cell Biol.* **61**, 387-394. doi:10.1139/o83-053

Vanderwaal, R. P., Maggi, L. B., Weber, J. D., Hunt, C. R. and Roti Roti, J. L. (2009). Nucleophosmin redistribution following heat shock: a role in heat-induced radiosensitization. *Cancer Res.* **69**, 6454-6462. doi:10.1158/0008-5472.CAN-08-4896

Vaughan, A., Alvarez-Reyes, M., Bridger, J. M., Broers, J. L., Ramaekers, F. C., Wehnert, M., Morris, G. E., Whitfield, W. GF. and Hutchison, C. J. (2001). Both emerin and lamin C depend on lamin A for localization at the nuclear envelope. *J. Cell Sci.* **114**, 2577-2590.

Velichko, A. K., Markova, E. N., Petrova, N. V., Razin, S. V. and Kantidze, O. L. (2013). Mechanisms of heat shock response in mammals. *Cell. Mol. Life Sci.* **70**, 4229-4241. doi:10.1007/s00018-013-1348-7

Villalobos, D. P., Bautista, R., Canovas, F. M. and Claros, M. G. (2004). Isolation of bacterial artificial chromosome DNA by means of improved alkaline lysis and double potassium acetate precipitation. *Plant Mol. Biol. Rep.* **22**, 1-7. doi:10.1007/BF02772684

Volpi, E. V., Chevret, E., Jones, T., Vatcheva, R., Williamson, J., Beck, S., Campbell, R. D., Goldsworthy, M., Powis, S. H., Ragoussis, J. et al. (2000). Large-scale chromatin organization of the major histocompatibility complex and other regions of human chromosome 6 and its response to interferon in interphase nuclei. *J. Cell Sci.* **113**, 1565-1576.

Williams, G. T. and Morimoto, R. I. (1990). Maximal stress-induced transcription from the human HSP70 promoter requires interactions with the basal promoter elements independent of rotational alignment. *Mol. Cell. Biol.* **10**, 3125-3136. doi:10.1128/MCB.10.6.3125

Williams, R. R. E., Broad, S., Sheer, D. and Ragoussis, J. (2002). Subchromosomal positioning of the epidermal differentiation complex (EDC) in keratinocyte and lymphoblast interphase nuclei. *Exp. Cell Res.* **272**, 163-175. doi:10.1006/excr.2001.5400

Willsie, J. K. and Clegg, J. S. (2002). Small heat shock protein p26 associates with nuclear lamins and HSP70 in nuclei and nuclear matrix fractions from stressed cells. *J. Cell. Biochem.* **84**, 601-614. doi:10.1002/jcb.10040

Wilson, K. L. and Foisner, R. (2010). Lamin-binding proteins. *Cold Spring Harb. Perspect. Biol.* **2**, a000554. doi:10.1101/cshperspect.a000554

Xie, W., Chojnowski, A., Boudier, T., Lim, J. S. Y., Ahmed, S., Ser, Z., Stewart, C. and Burke, B. (2016). A-type lamins form distinct filamentous networks with differential nuclear pore complex associations. *Curr. Biol.* **26**, 2651-2658. doi:10.1016/j.cub.2016.07.049

Yanoma, T., Ogata, K., Yokobori, T., Ide, M., Mochiki, E., Toyomasu, Y., Yanai, M., Kogure, N., Kimura, A., Suzuki, M. et al. (2017). Heat shock-induced HIKESHI protects cell viability via nuclear translocation of heat shock protein 70. *Oncol. Rep.* **38**, 1500-1506. doi:10.3892/or.2017.5844

Zastrow, M. S., Vlcek, S. and Wilson, K. L. (2004). Proteins that bind A-type lamins: integrating isolated clues. *J. Cell Sci.* **117**, 979-987. doi:10.1242/jcs.01102

Zhu, W.-G., Roberts, Z. V. and Dynlacht, J. R. (1999). Heat-induced modulation of lamin B content in two different cell lines. *J. Cell. Biochem.* **75**, 620-628. doi:10.1002/(SICI)1097-4644(19991215)75:4<620::AID-JCB8>3.0.CO;2-4

Zullo, J. M., Demarco, I. A., Piqué-Regi, R., Gaffney, D. J., Epstein, C. B., Spooner, C. J., Luperchio, T. R., Bernstein, B. E., Pritchard, J. K., Reddy, K. L. et al. (2012). DNA sequence-dependent compartmentalization and silencing of chromatin at the nuclear lamina. *Cell* **149**, 1474-1487. doi:10.1016/j.cell.2012.04.035

Supplementary Figure 1

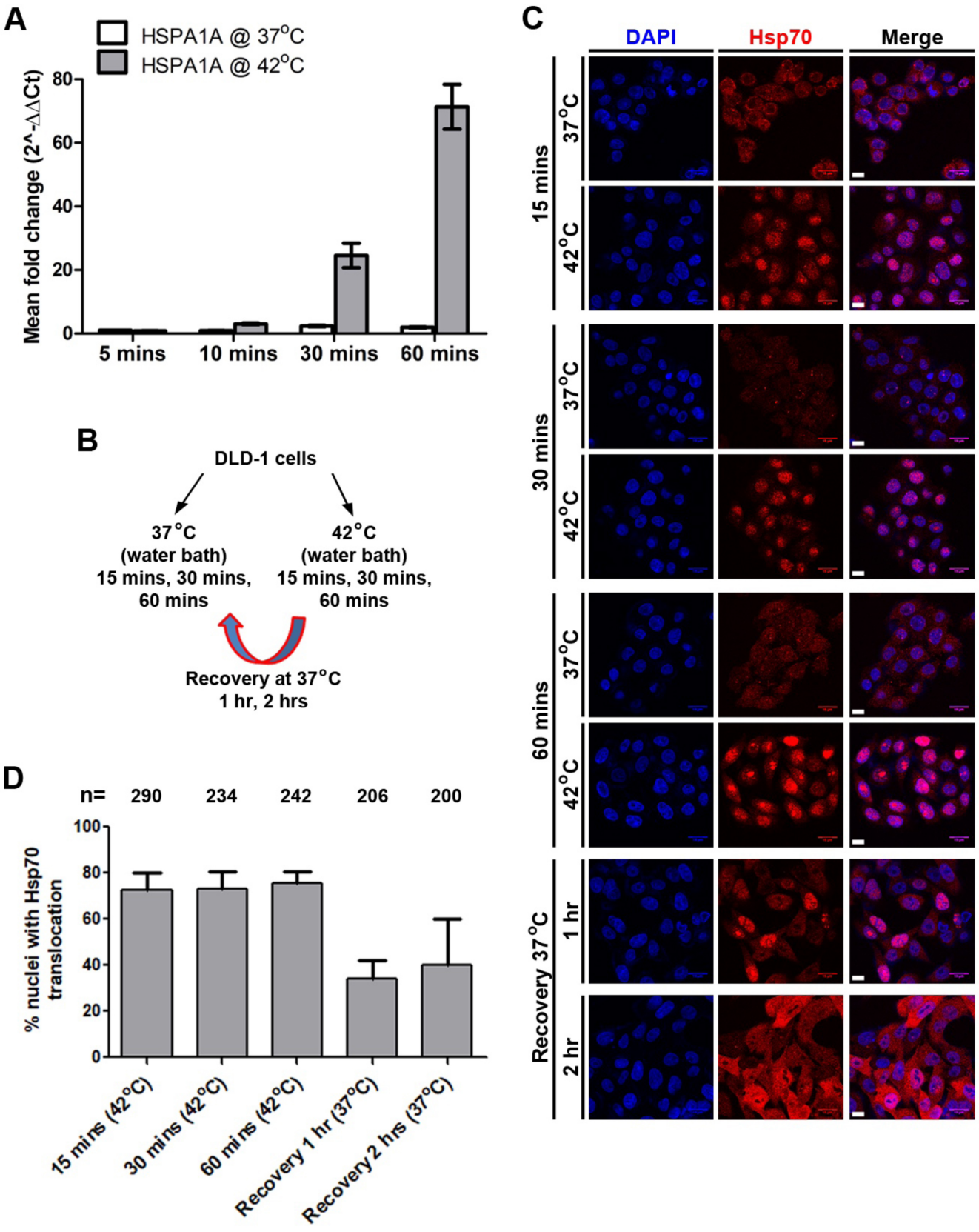

Figure S1.

A) Measurement of *HSPA1A* transcript levels using qRT-PCR in DLD-1 cells upon heat shock at 42^0C for 5, 10, 30 and 60 minutes. Combined data from N=2 independent biological replicates. Expression was first normalized to internal control – GAPDH and then to 37^0C/5 minutes. Error bar: SEM. *HSPA1A* transcript levels increase significantly over time from 5 minutes to 60 minutes.

B) Scheme for heat shock and recovery experiment.

C) Representative mid-optical sections from confocal z-stacks showing immunostaining of Hsp70 in DLD-1 cells exposed to heat shock at 42^0C for 15, 30, 60 minutes (same time points at 37^0C were used as controls) and cells under recovery for 1, 2 hrs at 37^0C post 60 minutes heat shock.

D) Quantification of % nuclei showing Hsp70 nuclear or nucleolar translocation after heat shock in cells exposed to heat shock at 42^0C for 15, 30, 60 minutes and cells under recovery for 1, 2 hrs at 37^0C post 60 minutes heat shock. Cells maintained at 37^0C show no nuclear translocation of Hsp70. Combined data from N=2 independent biological replicates. Error bar: SEM. n: number of nuclei. Scale bar ~10 µm.

Supplementary Figure 2

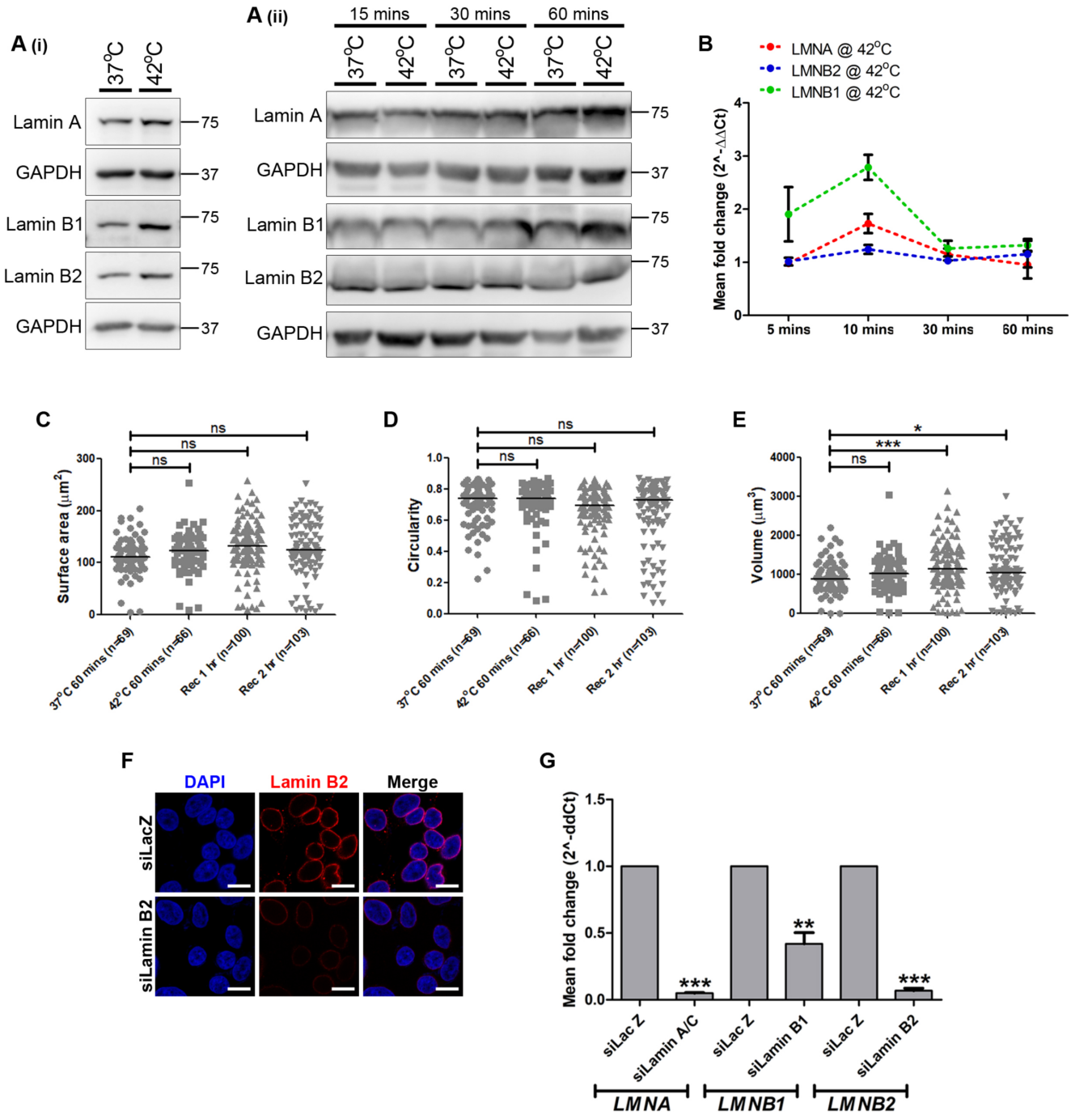

Figure S2.

A) (i) Representative western blots showing the expression levels of Lamin A, B1 and B2 in DLD-1 cells after heat shock at 42^0C for 60 minutes. GAPDH was used as a loading control *(N=2)*. (ii) Representative western blots showing the expression levels of Lamin A, B1 and B2 in DLD-1 cells after heat shock at 42^0C for 15, 30 and 60 minutes. GAPDH was used as a loading control *(N=2)*.

B) Measurement of *LMNA*, *LMNB1* and *LMNB2* transcript levels using qRT-PCR in DLD-1 cells upon heat shock at 42^0C for 5, 10, 30 and 60 minutes. Combined data from N=2 independent biological replicates. Expression was first normalized to internal control – GAPDH and then to respective 37^0C control. Error bar: SEM. Both *LMNA* and *LMNB1* expression is upregulated by 10 minutes of heat shock. *LMNB2* transcript levels are unaltered during heat shock.

C-E) Dot scatter plot representing nuclear surface area (C), nuclear circularity (D) and nuclear volume (E) in DLD-1 cells upon heat at 42^0C for 60 minutes, control cells at 37^0C and cells under recovery. Combined data from N=2 independent biological replicates. Black horizontal bar: Median (M). n: No. of nuclei. While no significant change is observed in either nuclear area or circularity upon heat shock, cells undergoing recovery from heat shock show an increase in nuclear volume (* $p<0.05$, *** $p<0.001$, Mann-Whitney test).

F) Representative mid-optical sections from confocal z-stacks confirming knockdown of Lamin B2 in DLD-1 cells treated with siRNA against Lamin B2 (For Fig. 3B). siLacZ treated cells were used as controls.

F) Measurement of *LMNA*, *LMNB1* and *LMNB2* expression using qRT-PCR in DLD-1 cells treated with either siLacZ, siLamin A/C, siLamin B1 or siLamin B2 (For Fig. 4B). Combined data from N=3 independent biological replicates. Error bar: SEM. Expression was first normalized to the internal control – GAPDH and then to the respective siLacZ control. (** $p<0.001$, *** $p<0.0001$, Student's t-test). Scale bar: ~10 µm.

Supplementary Figure 3

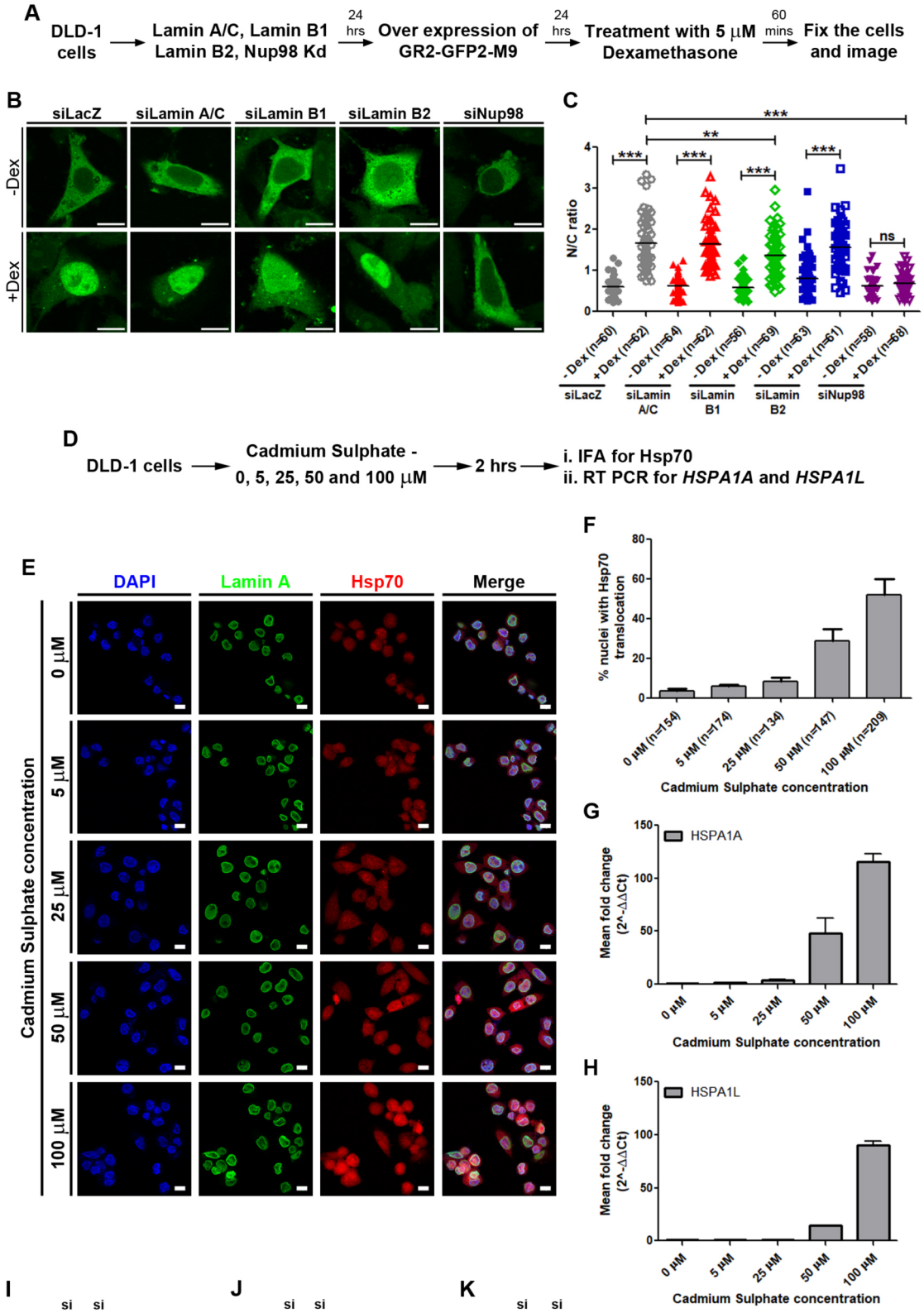

Figure S3.

A) Experimental scheme for nuclear import assay.

B) Representative confocal images showing the localization of GR2-GFP2-M9 in siLacZ, siLamin A/C, siLamin B1, siLamin B2 and siNup98 cells, with and without 5 µM dexamethasone treatment. The construct, which predominantly localizes in the cytoplasm, is imported into the nucleus following dexamethasone treatment.

C) Dot scatter plot showing the Nuclear/Cytoplasmic ratios of GR2-GFP2-M9 fluorescence intensities in siLacZ, siLamin A/C, siLamin B1, siLamin B2 and siNup98 cells, with and without 5 µM dexamethasone treatment. siLacZ, siLamin A/C and siLamin B2 cells show equivalent import of GR2-GFP2-M9, while siLamin B1 cells show a marginal reduction in the efficiency of import. Nup98 serves as a positive control, as depletion of Nup98 in DLD-1 cells abrogates nuclear import. ** $p<0.01$, *** $p<0.0001$ (Mann Whitney test).

D) Experimental scheme.

E) Representative mid-optical sections *(N=2)* from confocal z-stacks showing immunostaining of Lamin A and Hsp70 in DLD-1 cells treated with increasing concentration of cadmium sulphate (0 µM – 100 µM) for 2 hrs. Maximum volume of nuclease free water was used as control (0 µM).

F) Quantification of % nuclei showing Hsp70 nuclear or nucleolar translocation after treatment with increasing concentration of cadmium sulphate (0 µM – 100 µM) for 2 hrs. NFW control (0 µM) showed no nuclear translocation of Hsp70. Combined data from N=2 independent biological replicates. n: No. of nuclei. Hsp70 nuclear translocation shows a dose dependent increase with cadmium sulphate concentrations.

G) Measurement of *HSPA1A* expression using qRT-PCR in DLD-1 cells after treatment with increasing concentration of cadmium sulphate (0 µM – 100 µM) for 2 hrs. Expression was first normalized to internal control – GAPDH and then to 0 µM (NFW control). Combined data from N=2 independent biological replicates. Error bar: SEM. *HSPA1A* transcript levels show a dose dependent increase with cadmium sulphate concentrations.

H) Measurement of *HSPA1L* expression using qRT-PCR in DLD-1 cells after treatment with increasing concentration of cadmium sulphate (0 µM – 100 µM) for 2 hrs. Expression was first normalized to internal control – GAPDH and then to 0 µM (NFW control). Combined data from N=2 independent biological replicates. Error bar: SEM. *HSPA1L* transcript levels show a dose dependent increase with cadmium sulphate concentrations.

I-K) Representative western blots confirming siRNA mediated knockdown of Lamin A (B), Lamin B2 (C) and Lamin B1 (D). GAPDH was used as a loading control (For Fig. 4D-E). Scale bar: ~10 µm.

Supplementary Figure 4

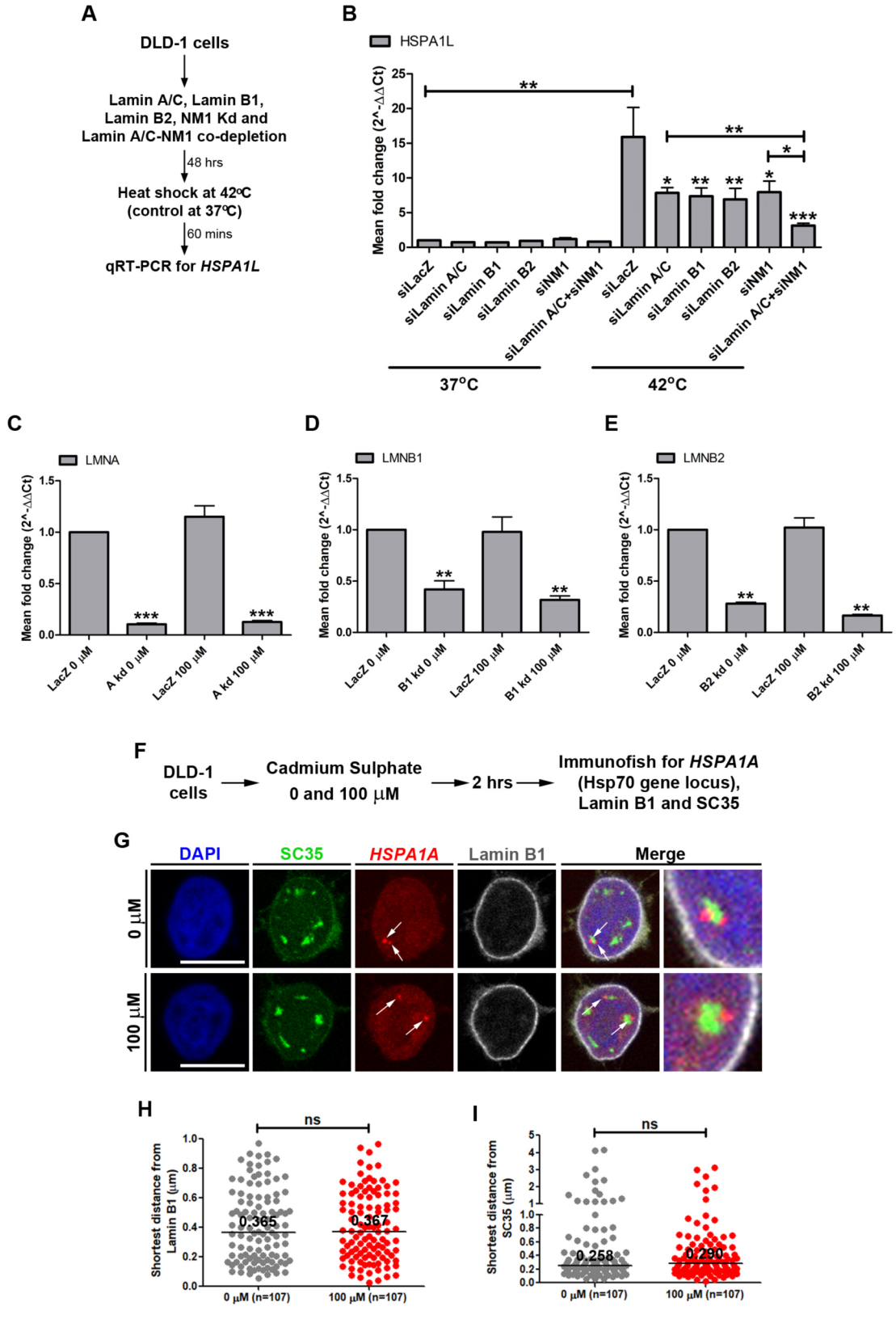

Figure S4.

A) Experimental scheme for analyzing *HSPA1L* transcript levels.

B) Measurement of *HSPA1L* transcript levels in cells with single depletions of Lamin A/C, Lamin B1, Lamin B2, NM1 and co-depletion of Lamin A/C and NM1, subjected to heat shock at 42ºC for 60 minutes. siLacZ treated cells were used as controls. Expression was first normalized to internal control – GAPDH and then to siLacZ 37ºC. Combined data from N=2 independent biological replicates. Error bar: SEM. * $p<0.05$, ** $p<0.01$, *** $p<0.0001$ (Student's t test). Heat shock induced upregulation of *HSPA1L* expression is attenuated in siLamin A/C, siLamin B1, siLamin B2 and siNM1 cells and cells with co-depletion of Lamin A/C and NM1 show an additive effect on *HSPA1L* repression.

C-E) Measurement of *LMNA* (C), *LMNB1* (D) and *LMNB2* (E) transcript levels using qRT-PCR in DLD-1 cells treated with either siLacZ, siLamin A/C, siLamin B1 or siLamin B2 and 100 µM cadmium sulphate for 2 hrs (For Fig. 4C). Combined data from N=3 independent biological replicates. Expression was first normalized to internal control – GAPDH and then to siLacZ 0 µM. Error bar: SEM. (** $p<0.001$, *** $p<0.0001$, Student's t-test).

F) Experimental scheme.

G) Representative mid-optical sections *(N=2)* from confocal z-stacks showing SC35 and Lamin B1 immunostaining, and 3D-FISH for Hsp70 gene locus in cells treated with 100 µM cadmium sulphate for 2 hours. White arrows: Specific hybridization of BAC DNA probe showing 2 copies of Hsp70 gene locus.

H) Dot scatter plot showing the shortest distance of the Hsp70 loci from Lamin B1 staining in cells treated with 100 µM cadmium sulphate for 2 hours. Combined data from N=2 independent biological replicates. Black horizontal bar: Median (M). n: No. of loci. Hsp70 gene loci do not show repositioning with respect to the nuclear lamina upon cadmium sulphate treatment (Mann- Whitney test).

G) Dot scatter plot showing the shortest distance of the Hsp70 loci from SC35 speckles in cells

treated with 100 µM cadmium sulphate for 2 hours. Combined data from N=2 independent biological replicates. Black horizontal bar: Median (M). n: No. of loci. Hsp70 gene loci do not show repositioning with respect to the SC35 nuclear speckles upon cadmium sulphate treatment (Mann-Whitney test). Scale bar: ~10 µm.

Supplementary Figure 5

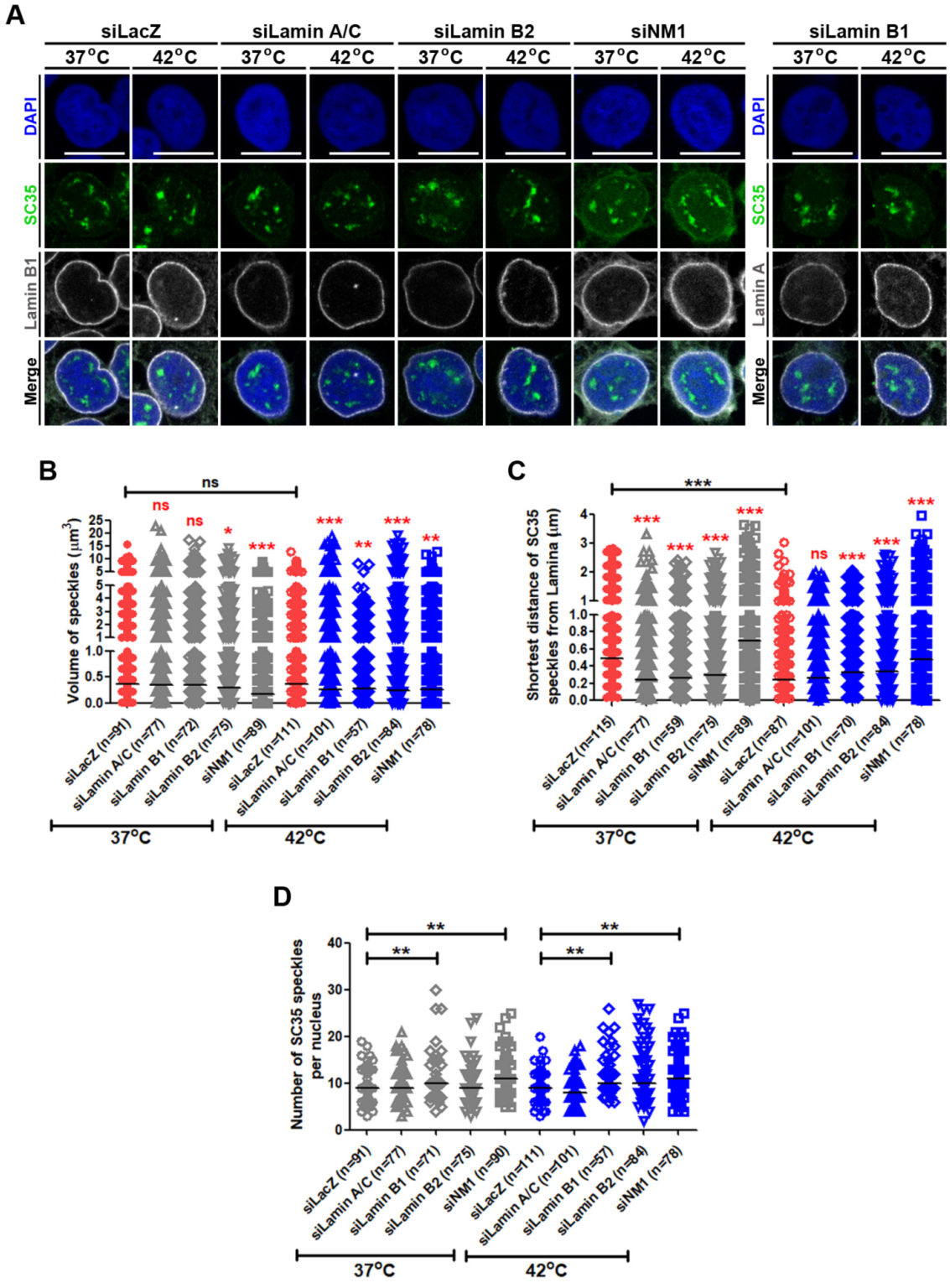

Figure S5

A) Representative mid-optical sections *(N=2)* from confocal z-stacks showing SC35 and Lamin B1 or Lamin A immunostaining in siLacZ, siLamin A/C, siLamin B1, siLamin B2 and siNM1 cells subjected to heat shock at 42ºC for 60 minutes.

B) Dot scatter plot showing the volumes of individual SC35 speckles siLacZ, siLamin A/C, siLamin B1, siLamin B2 and siNM1 cells subjected to heat shock at 42ºC for 60 minutes. Combined data from N=2 independent biological replicates. Black horizontal bar: Median (M). n: No. of nuclei. * $p<0.05$, ** $p<0.01$, *** $p<0.0001$ (Mann Whitney test). siLacZ cells do not show a significant change in median SC35 speckle volume upon heat shock. Lamin A/C and B1 depletion only reduces speckle volume upon heat shock, while siLamin B2 and siNM1 cells show smaller SC35 speckles at both 37ºC and 42ºC.

C) Dot scatter plot showing the shortest distance of individual SC35 speckles from nuclear lamina in siLacZ, siLamin A/C, siLamin B1, siLamin B2 and siNM1 cells subjected to heat shock at 42ºC for 60 minutes. Combined data from N=2 independent biological replicates. Black horizontal bar: Median (M). n: No. of nuclei. *** $p<0.0001$ (Mann Whitney test). siLacZ cells show a redistribution of SC35 speckles toward the nuclear periphery upon heat shock. Loss of either of the lamins shows a similar repositioning of the speckles toward the nuclear periphery even in the absence of heat shock, while Lamin B1 and B2 knockdown curtails this movement upon heat shock. siNM1 cells show repositioning of SC35 speckles toward the nuclear interior at both 37ºC and 42ºC.

D) Dot scatter plot showing the number of SC35 speckles per nucleus in siLacZ, siLamin A/C, siLamin B1, siLamin B2 and siNM1 cells subjected to heat shock at 42ºC for 60 minutes. Combined data from N=2 independent biological replicates. Black horizontal bar: Median (M). n: No. of nuclei. ** $p<0.01$ (Mann Whitney test). Knockdown of either Lamin B1 or NM1 leads to a marginal increase in the number of speckles per nucleus. Scale bar: ~10 µm.

Supplementary Figure 6

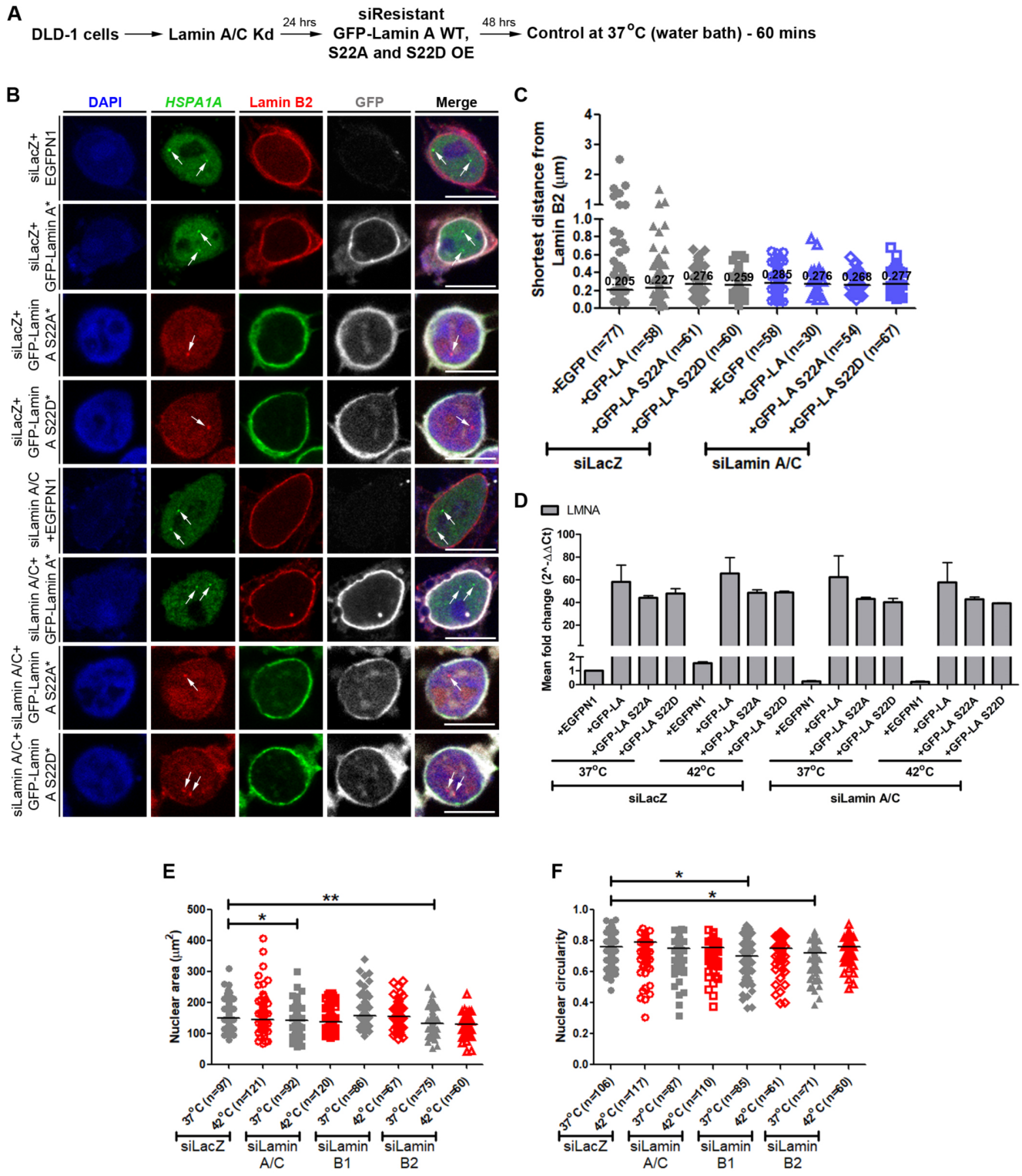

Figure S6.

A) Experimental scheme depicting overexpression of siRNA resistant GFP-Lamin A.

B) Representative mid-optical sections from confocal z-stacks showing immunostaining of Lamin B2 and GFP, and 3D-FISH for Hsp70 gene locus in siLacZ or siLamin A/C cells overexpressing EGFP-N1, siRNA resistant GFP-Lamin A (GFP-Lamin A*) WT, S22A or S22D at 37^0C for 60 minutes. White arrows: Specific hybridization of BAC DNA probe showing 2 copies of Hsp70 gene locus.

C) Dot scatter plot representing the shortest distance of the Hsp70 loci from Lamin B2 staining in siLacZ or siLamin A/C cells overexpressing EGFP-N1, siRNA resistant GFP-Lamin A (GFP-Lamin A*) WT, S22A or S22D at 37^0C for 60 minutes. *(N=1).* Black horizontal bar: Median (M). n: No. of loci. Overexpression of GFP-Lamin A WT, S22A or S22D does not affect the spatial positions of the Hsp70 gene locus in cells at 37ºC (Mann-Whitney test).

D) Measurement of *LMNA* transcript levels using qRT-PCR in siLacZ and siLamin A/C cells, overexpressing EGFP-N1, siRNA resistant GFP-Lamin A WT, S22A or S22D and subjected to heat shock at 42ºC for 60 minutes. Expression was normalized to internal control – GAPDH and then to siLacZ+EGFP-N1/37^0C control. (Combined data from N=2 independent biological replicates, Error bar: SEM).

E) Dot scatter plot showing nuclear areas of siLacZ, siLamin A/C, siLamin B1 and siLamin B2 cells subjected to heat shock at 42ºC for 60 minutes. Combined data from N=2 independent biological replicates. Black horizontal bar: Median (M). n: No. of nuclei. Lamin A/C knockdown shows a marginal decrease, while Lamin B2 knockdown shows a significant decrease in the nuclear area. * $p<0.05$, ** $p<0.01$ (Mann Whitney test).

F) Dot scatter plot showing nuclear circularity of siLacZ, siLamin A/C, siLamin B1 and siLamin B2 cells subjected to heat shock at 42ºC for 60 minutes. Combined data from N=2 independent biological replicates. Black horizontal bar: Median (M). n: No. of nuclei. Lamin B1 and B2 knockdown shows a marginal decrease in the nuclear circularity. * $p<0.05$, ** $p<0.01$ (Mann Whitney test). Scale bar: ~10 µm.

Supplementary Figure 7

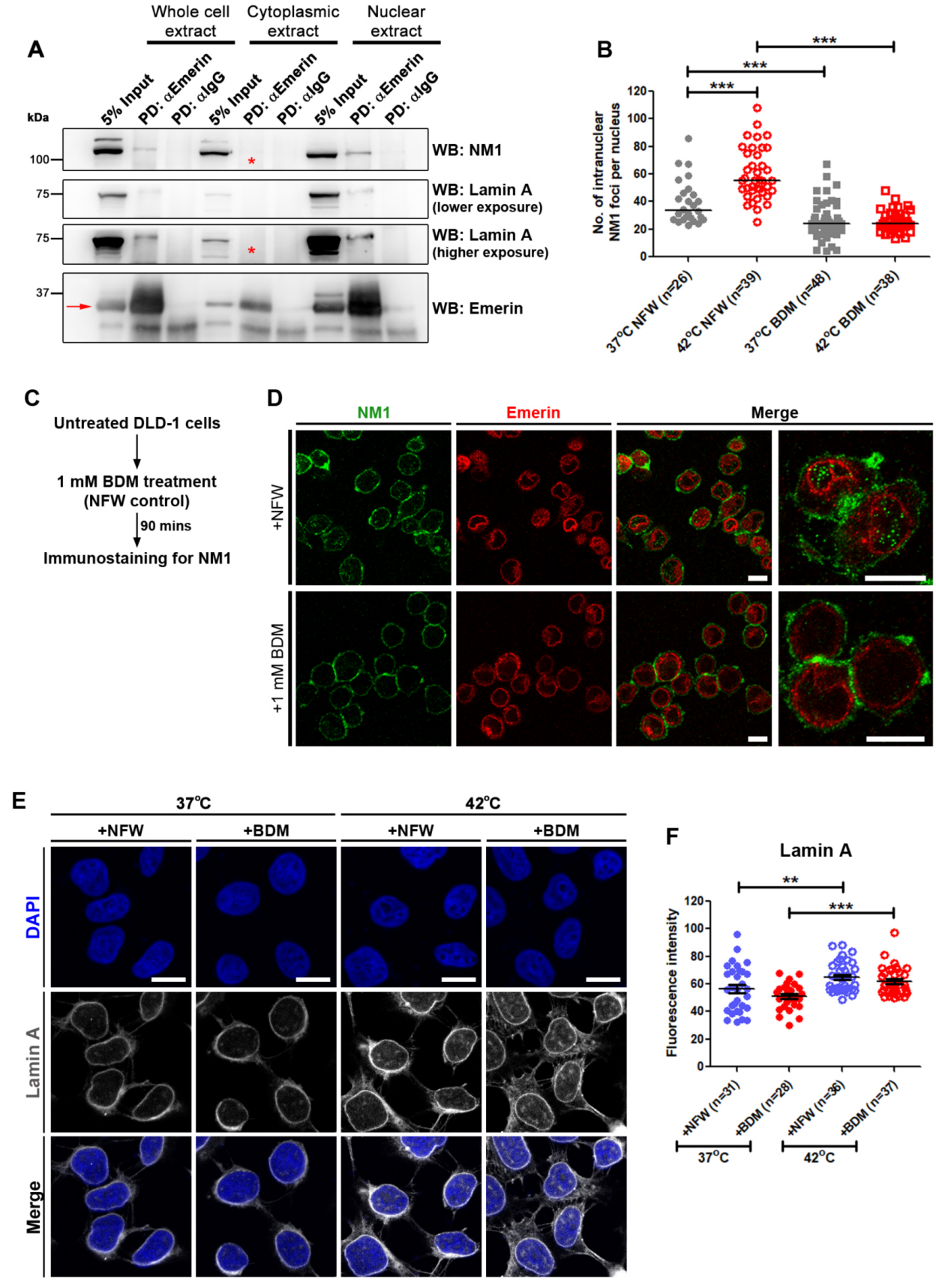

Figure S7

A) Representative Co-IP *(N=2)* using anti-Emerin antibody (red arrow), probed for interaction with NM1 and Lamin A in whole cell, cytoplasmic and nuclear extracts of DLD-1 cells. The tripartite Lamin A-Emerin-NM1 complex is detected only in the whole cell and nuclear extracts.

B) Dot scatter plot showing the number of intranuclear NM1 foci per nucleus in cells treated with BDM and subjected to heat shock at 42^{o}C for 60 minutes. Equal volume of nuclease free water (NFW) was used as control. Data from a single experiment. While control cells (+NFW) show an increase in the number of intranuclear NM1 foci per nucleus upon heat shock, BDM treated cells show a significant reduction in NM1 foci numbers at 37^{o}C and 42^{o}C. Black horizontal bar: Median (M). n: No. of nuclei. *** $p<0.0001$ (Mann Whitney test).

C) Experimental scheme for BDM treatment of control DLD-1 cells.

D) Immunostaining for NM1 and Emerin in DLD-1 cells treated with 1 mM BDM (or equal volume of nuclease free water) to confirm depletion of intranuclear NM1 foci and inhibition of NM1.

E) Representative mid-optical sections from confocal z-stacks showing immunostaining of Lamin A in DLD-1 treated with 1 mM BDM (or equal volume of nuclease free water).

F) Dot scatter plot of normalized fluorescence intensities (from line scan analysis of each individual nucleus) for Lamin A in cells treated with 1 mM BDM (or equal volume of nuclease free water). Data from a single experiment. Black horizontal bar: Mean ±SEM. n: No. of nuclei. BDM treatment does not affect the basal expression of Lamin A or the heat shock induced upregulation of Lamin A. ** $p<0.001$, *** $p<0.0001$ (Mann-Whitney test). Scale bar: ~10 µm.

Supplementary Figure 8

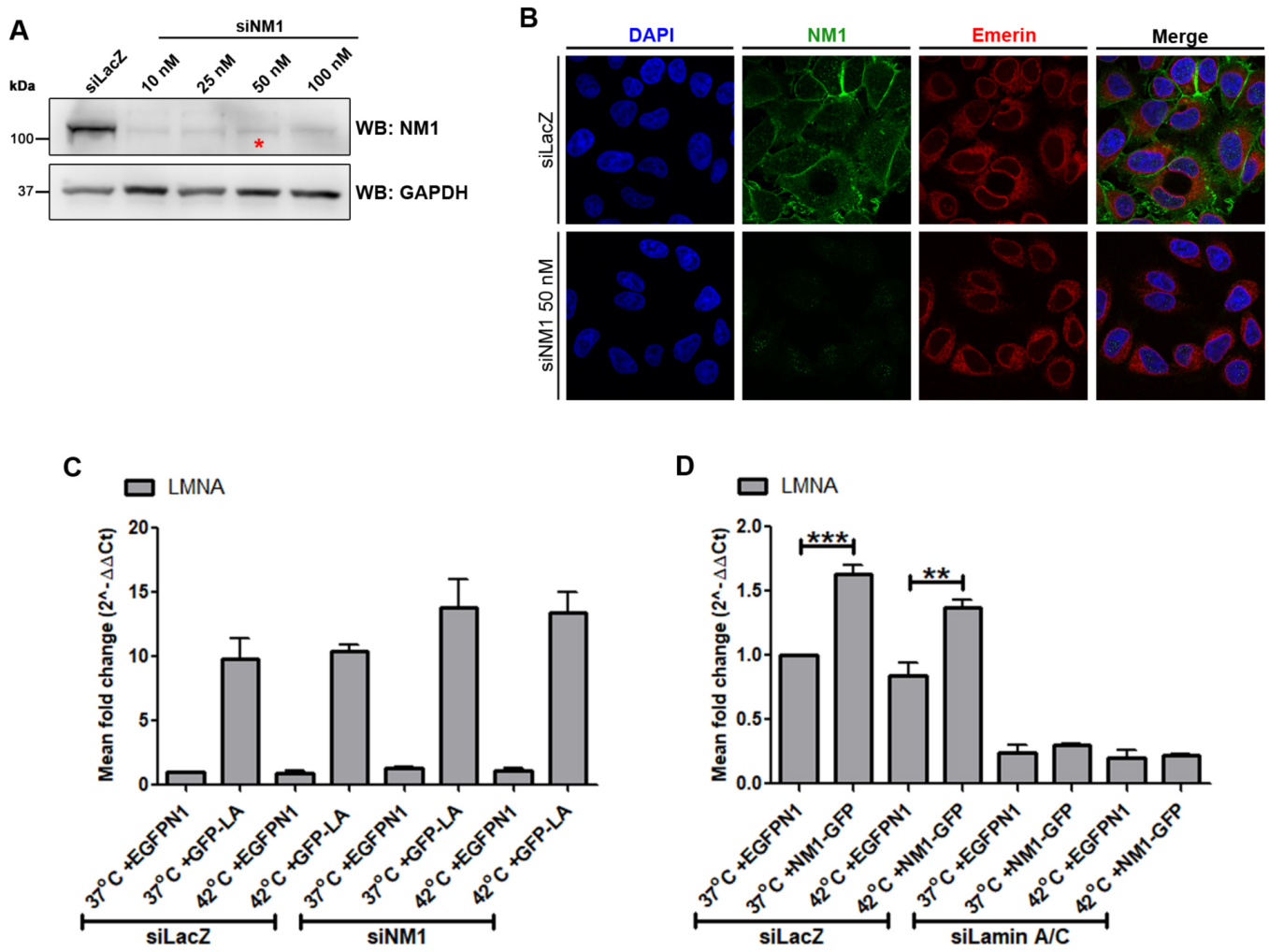

Figure S8.

A) Representative western blots confirming the siRNA mediated knockdown of NM1 in DLD-1 cells. Although downregulation of NM1 is observed from 10 nM siRNA, further experiments were performed using 50 nM NM1 siRNA (red asterisk) to achieve a homogenous cell population showing NM1 knockdown.

B) Representative mid-optical sections from confocal z-stacks showing immunostaining of NM1 and Emerin in siNM1 cells. siRNA mediated knockdown of NM1 leads to a near-complete absence of NM1.

C) Measurement of *LMNA* transcript levels using qRT-PCR in siLacZ and siNM1 cells, overexpressing EGFP-N1 or GFP-Lamin A and subjected to heat shock at 42^{o}C for 60 minutes. Expression was normalized to internal control – GAPDH and then to siLacZ+EGFP-N1/37^{0}C control. (Combined data from N=2 independent biological replicates, Error bar: SEM).

D) Measurement of *LMNA* transcript levels using qRT-PCR in siLacZ and siLamin A/C cells, overexpressing EGFP-N1 or NM1-GFP and subjected to heat shock at 42^{o}C for 60 minutes. Expression was normalized to internal control – GAPDH and then to siLacZ+EGFP-N1/37^{0}C control (Combined data from N=2 independent biological replicates, Error bar: SEM).

Table S1: List of siRNAs used in the study

si*LACZ*	5’ CGUACGCGGAAUACUUCGA 3’
si*LMNA/C*	5’ CAGUCUGCUGAGAGGAACA 3’
si*LMNB1*	5’ AGACAAAGAGAGAGAGAUG 3’
si*LMNB2*	5’ GAGCAGGAGAUGACGGAGA 3’
siNM1	ON-TARGETplus SMARTpool-Human MYO1C L-015121-00-0005

Table: S2: List of Primers for creating mutant Lamin A/C

siResistant Lamin A F	5’CTGGACAATGCCAGGCAATCCGCCGAAAGAAATAGCAACCTGGTGGGG 3’
siResistant Lamin A R	5’CCCCACCAGGTTGCTATTTCTTT 3’
Lamin A S22A F	5'-GCGGGTGGGCGCCAGCGGAGTGG-3'
Lamin A S22A R	5'-CCACTCCGCTGGCGCCCACCCGC-3'
Lamin A S22D F	5'-GGTGATGCGGGTGGGATCCAGCGGAGTGGAGCT-3'
Lamin A S22D R	5'-AGCTCCACTCCGCTGGATCCCACCCGCATCACC-3'

Table S3: List of Antibodies used in this study

Rabbit anti-Lamin A (ab26300)	IFA 1:500, WB 1:1000
Rabbit anti-Lamin B1 (ab16048)	IFA 1:500, WB 1:1000
Mouse anti-Lamin B2 (ab8980)	IFA 1:400, WB 1:500
Rabbit anti-GAPDH (Sigma G9545)	WB 1:5000
Rabbit anti-MYO1C (ab51261)	IFA 1:75
Rabbit anti-Myosin 1β (nuclear, M3567)	WB 1:1000
Sheep anti-mouse IgG-HRP (NA9310V)	WB 1:10000
Donkey anti-rabbit IgG HRP (NA9340V)	WB 1:10000
Rabbit anti-GFP (Sigma G1455)	IFA 1:400
Goat anti-Rabbit Alexa-488 (A11034)	IFA 1:1000
Goat anti-Mouse Alexa-568 (A11004)	IFA 1:1000
Goat anti-Rabbit Alexa-568 (A11011)	IFA 1:1000
Goat anti-Mouse Alexa-488 (A11001)	IFA 1:1000
Goat anti-Rabbit Alexa-647 (ab150075)	IFA 1:1000

Table: S4: List of primers used in the study

LMNA/C F	5'CCGCAAGACCCTTGACTCA 3'
LMNA/C R	5'TGGTATTGCGCGCTTTCAG 3'
LMNB2 F	5'AGTTCACGCCCAAGTACATC 3'
LMNB2 R	5'CTTCACAGTCCTCATGGCC 3'
LMNB1 F	5'CGACCAGCTGCTCCTCAACT 3'
LMNB1 R	5'CTTGATCTGGGCGCCATTA 3'
HSPA1A F	5'AGAAGGACGAGTTTGAGCACA 3'
HSPA1A R	5'TGGTACAGTCCGCTGATGATG 3'
HSPA1L F	5'TACCGTGCCAGCCTATTTCAA3'
HSPA1L R	5'AGCAATCACACCTGCATCCTT3'
GAPDH F	5'CGAGATCCCTCCAAAATCAAG 3'
GAPDH R	5'GCAGAGATGATGACCCTTTTG 3'